Characterisation of N-terminal fragments of Retinoblastoma Binding Protein 6 for structural analysis

Matodzi Portia Maumela

A thesis submitted in fulfilment of the requirements for the Degree Magister Scientiae in the Department of Biotechnology, Faculty of Science, University of the Western Cape

UNIVERSITY *of the* WESTERN CAPE

Supervisor: Dr David JR Pugh

January 2016

Abstract

**Characterisation of N-terminal fragments of Retinoblastoma Binding Protein 6
for structural analysis**

P. Maumela, MSc (Biotechnology) Thesis, Department of Biotechnology, Faculty of Science,
University of the Western Cape

Retinoblastoma Binding Protein 6 (RBBP6) is a 200 kDa RING finger-containing protein that plays a role in 3'-end poly-adenylation of mRNA transcripts as well as acting as an E3 ubiquitin ligase against a number of proteins involved in tumourigenesis, including p53. Since the human protein is too large and poorly structured for heterologous expression in bacteria, it would be advantageous to identify smaller fragments suitable for expression in bacteria. Many E3 ubiquitin ligases form homo-dimers and dimerisation is important for their activity; structural studies of the isolated RING finger of RBBP6 showed that it forms a weak homo-dimer. This poses the question of whether the complete RBBP6 protein forms homo-dimers *in vivo*, and, if so, whether a fragment of RBBP6 containing the RING finger could be identified which would be suitable for structural as well as functional studies. Such a construct would allow detailed investigation of the homo-dimeric state of the fragment, the relationship between dimerisation and ubiquitination activity, and the role of domains such as the DWNN domain and zinc finger in ubiquitination.

A fragment consisting of the first 335 residues of RBBP6, dubbed R3 because it contained the first three domains of the protein, was expressed, along with three variants expressing mutations known to disrupt the dimerisation of the isolated RING finger. Size exclusion chromatography showed that R3 forms a strong homo-dimer that was not disrupted by the mutations, suggesting that additional parts of R3 outside of the isolated RING finger form part of the interface. To identify whether this included the DWNN domain or the zinc finger, a shorter fragment dubbed R2, excluding the N-terminal DWNN domain, was cloned and expressed. This was also found to form a strong homo-dimer, suggesting that the DWNN domain may not form an essential part of the dimer interface.
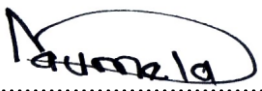
Availability of the RING finger samples and monomerising mutations allowed investigation of whether the RING finger from RBBP6 was able to auto-ubiquitinate itself. Using a fully *in vitro* ubiquitination assay supplemented with intact proteasomes purified from human cell lysates, we found that wild type RING auto-ubiquitinates itself very efficiently, catalysing its own destruction in the proteasome. This provides an answer to the question of why RBBP6 is so difficult to detect in mammalian cells. Surprisingly, monomeric mutant RING fingers were also able to auto-ubiquitinate and catalyse their own destruction, although perhaps not as efficiently as wild type. This result would appear to rule out the hypothesis that dimerisation of RBBP6 is required for ubiquitination activity. Finally, samples of the RING finger from human MDM2 were expressed in bacteria and used to investigate whether the RING fingers of RBBP6 and MDM2 interact directly with each other. If so, this may provide a mechanism whereby RBBP6 and MDM2 cooperate in ubiquitination of p53. The results of a GST pull down assay using GST-MDM2-RING as "bait" and RBBP6-RING as "prey" provides evidence that such an interaction between the RING does exist. This work lays the foundation for future structural studies of the RING-RING hetero-dimer using protein Nuclear Magnetic Resonance Spectroscopy.

Keywords: Cancer, RBBP6, MDM2, p53, ubiquitination, proteasome, size exclusion chromatography, GST pull down, Western Blot

Declaration

I declare that "Characterisation of N-terminal fragments of Retinoblastoma Binding Protein 6 for structural analysis" is my own work that has not been submitted for any degree or examination in any other university, and that all the sources I have used or quoted have been indicated or acknowledged by complete references.

Matodzi Portia Maumela

Signature:.................................... Date: January 2016

Acknowledgments

It is a great honour and happiness to say thank you to Dr David Pugh for the opportunity and the serene space he gave me during the years as I served as Masters student in his laboratory. He might not imagine, but this opportunity granted tremendous growth to me in different areas of life. I became more conscious of many things I would otherwise have missed out on; for example, the biotechnology techniques and communication skills I have learned. It also made me to tap into the different ways of critical thinking and it was fascinating to see how changeling research can be. The ability to troubleshoot whenever an experiment was unsuccessful, communicate with my colleagues (especially Andrew Faro); listening to their inputs and ideas, I personally treasure this experience.

I uphold the Graduate Attributes of the University of the Western Cape with pride, because of Dr Pugh's laboratory that has allowed me to be critically towards knowledge and be a lifelong learner with an attitude and stance toward myself.

As I say thanks for these years, I must also acknowledge that it was not a bed of roses, it was challenging, but I thank my family, including my husband Siphiwe Makhubu and my parents Joyce Maumela and Edison Maumela for their support, encouraging words and ever jovial and happy attitude that kept me motivated. I also like to thank my family as a whole for being there for me during the course of my masters.

I am grateful to the National Research Foundation of South Africa for providing the necessary financial support.

To conclude I will like to thank the ALMIGHTY, who made all the opportunities possible, and who directed me to the best laboratory and for a wonderful family.
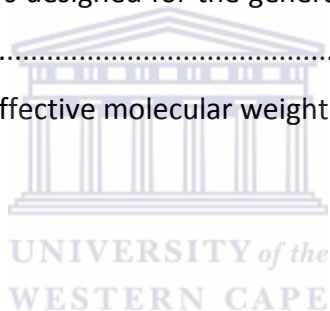
Abbreviations

Amp	Ampicillin
APS	Ammonium persulphate
Asn or N	Asparagine
ATP	Adenosine tri-phosphate
bp	Base pairs
BSA	Bovine serum albumin
C-terminus	Carboxyl terminus
Cm	Chloramphenicol
CV	Column volume
Da	Dalton
DNA	Deoxyribonucleic acid
dNTP	Deoxynucleotide
DWNN	Domain with no name
DTT	Dithiothreitol
E1	Ubiquitin activating enzyme
E2	Ubiquitin conjugating enzyme
E3	Ubiquitin ligase
Glu or E	Glutamic acid
GST	Glutathione S-transferase
Fig	Figure
HDM2	Human double minute 2
His or H	Histidine
IPTG	Isopropyl β-D-1-thiogalactopyranoside
Kan	Kanamycin
Kbp	Kilobase pair
kDa	Kilodaltons
LB	Luria Bertani broth
Lys or K	Lysine
MDM2	Mouse double minute

Mg.ATP	ATP magnesium salt
MW	Molecular weight
N-terminus	Amino terminus
ng	Nanogram
μl	Microliter
p53	Protein 53
PAGE	Polyacrylamide gel electrophoresis
PBS	Phosphate buffered saline
PCR	Polymerase chain reaction
PVDF	Polyvinyldifluoride
RBBP6	Retinoblastoma binding protein 6
RING	Really interesting new gene
SDS	Sodium dodecyl sulphate
SV40	Simian virus 40
TBS	Tris buffered saline
TEMED	*N,N,N',N'*-tetramethylethylenediamine
Tfb	Transformation buffered
Tris	2-amino-2-hydroxymethylpropane-1, 3-diol
UV	Ultraviolet
YB-1	Y-box binding protein 1
Zn^{2+}	Zinc ion
$ZnSO_4$	Zinc Sulphate

List of Table

UNIVERSITY *of the*

WESTERN CAPE

List of Figures

Table of Contents

Chapter 1: Literature Review

1.1 Gene structure and domain structure of RBBP6

Fragments of Retinoblastoma Binding Protein 6 (RBBP6) were independently identified by different groups and given a number of different names: Retinoblastoma Binding Q protein 1 (RBQ-1) corresponds to residues 150-1146, p53-associated cellular protein testes derived (PACT) corresponds to residues 207-1792, and proliferation potential-related protein (P2P-R or PP-RP) corresponds to residues 199-1792 of the 1792-residue human protein (Sakai *et al.* 1995, Simons *et al.* 1997; Witte and Scott 1997)**.**

In humans, the single copy RBBP6 gene is found on chromosome 16p12.2 encoding for three protein isoforms due to alternative splicing and poly-adenylation (Sakai *et al.* 1995; Gao and Scott 2002; Gao *et al.* 2002). Three mRNA transcripts of this gene are expressed, namely, 1.1, 6.0, and 6.1 Kb transcripts. The 6.1 kb transcript encodes the longest isoform of 1792-residues known as isoform 1; isoform 2 corresponds to an alternative splicing transcript of 6.0 kb and codes for a protein of 1758-residues. The 1.1 kb transcript is expressed from an alternative promoter and codes for a 118-residue protein known as isoform 3. The respective sequences of the different isoforms are Genbank: NP_008841, Genbank: NP_061173 and Genbank: NP_116015.

RBBP6 orthologues are found in all eukaryotes, but not in prokaryotes. RBBP6 is a multi-domain protein; the organization of the domains in different eukaryotic organisms is shown in Figure 1.1. A minimal isoform containing the three N-terminal domains, the DWNN domain, the zinc knuckle, and the RING finger, is found in all RBBP6 orthologues (Pugh *et al.* 2006). In higher eukaryotes such as human, RBBP6 isoforms contain additional C-terminal domains, including an SR-like domain, as well as domains identified in humans as binding pRb and p53 respectively (Witte and Scott 1997; Simons *et al.* 1997; Yoshitake *et al.* 2004; Pugh *et al.* 2006).
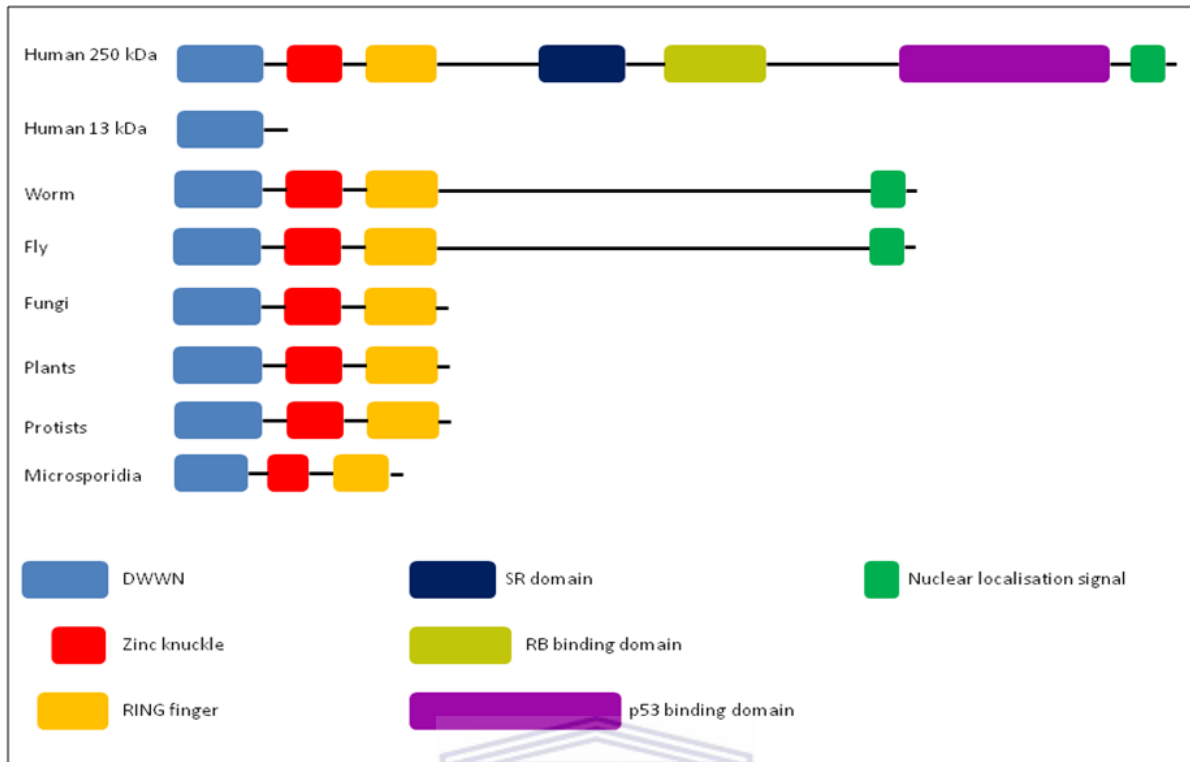
Figure 1.1: Domain structure of Retinoblastoma Binding Protein 6 (RBBP6). The first three N-terminal domains - the DWNN domain, zinc finger and RING finger - are found in all RBBP6 homologues, including human, plants, worm, fly, fungi, protists, and microsporidia. In humans, 13 kDa DWNN is also expressed independently, including a C-terminal tail not present in the full-length protein. Additional domains to the first three N-terminal domains, including the SR-like domain, RB binding domain, p53 binding domain and nuclear localization signal are found in higher eukaryotes such as human (Pugh *et al.* 2006).

1.2 The role of RBBP6 in mRNA processing

RBBP6 forms part of the cleavage and poly-adenylation factor complex in yeast and the pre-mRNA 3'-end processing complex in humans (Vo *et al.* 2001; Shi *et al.* 2009). Post-transcriptional cleavage of mRNA precursors is an essential step in the synthesis of functional eukaryotic mRNAs. Following cleavage, most eukaryotic mRNAs acquire a poly(A) tail at their 3'-ends. Poly(A) tails are directly implicated in the regulation of gene expression because they have a profound influence on the stability, export, and translation efficiency of mRNAs. Large pre-mRNA 3'-end processing complexes are required to reconstitute the complete poly-adenylation process (Colgan and Manley 1997; Zhao *et al.* 1999). Along with other proteins, including WDR33 (a WD40 repeat-containing protein and a putative mammalian homologue of the yeast 3'-end processing factor Pfs2) and PP1 (serine/threonine phosphatase), RBBP6 is implicated in mRNA 3'-end processing in mammals and is a known homologue of yeast 3'-end processing factor Mpe1. Mpe1 is a

subunit of the cleavage and poly-adenylation factor (CPF) complex. This complex is responsible for the specific cleavage and poly-adenylation of pre-mRNA (Vo *et al*. 2001; Shi *et al*. 2009).

Like RBBP6, Mpe1 contains the DWNN domain, the zinc knuckle and the RING finger. The DWNN domain of Mpe1 is essential for the association of Mpe1 with CPF and CF IA and the RING finger contributes to the interaction with CPF but not to that with CF IA. While the zinc knuckle of Mpe1 or the second linker region also makes contact with other CPF subunits. These three domains are needed for optimal cell growth and function in mRNA 3'-end processing. Both the zinc knuckle and RING finger domains are essential for efficient binding of Mpe1 to RNA (Lee and Moore 2014).

RBBP6 is significantly larger than Mpe1 and contains additional domains, including an arginine/serine-rich (RS) domain that is found in many splicing factors. The ubiquitin-like DWNN domain of RBBP6 has been shown to interact with two of the seven core splicing proteins, SmB (Simons *et al*, 1997) and SmG (Pugh *et al.* 2006, Kappo *et al*. 2012). RBBP6 may link mRNA 3'-end formation to the Rb/p53 pathways and tumorigenesis (Shi *et al*. 2009). RBBP6 and isoform 3 (DWNN) regulate the 3'-end processing of RNAs with AU-rich 39 un-translated regions (UTRs) such as c-Fos and c-Jun. Unlike RBBP6-N, a fragment containing only the DWNN domain, zinc knuckle and RING finger, a derivative (ΔDWNN) lacking the DWNN domain was unable to reconstitute cleavage activity, indicating that the DWNN domain is essential in 3'-end processing. However, DWNN inhibits the binding to RNA because ΔDWNN shows enhanced RNA-binding affinity. Isoform 3 outcompetes RBBP6 for binding to CstF, thus inhibiting cleavage of SVL pre-mRNA (Di Giammartino *et al*. 2014).

The tertiary structure of DWNN is almost superimposable onto ubiquitin, suggesting that DWNN may act as an ubiquitin-like modifier (Pugh *et al*. 2006). As the first step in the process of ubiquitination, a specific protease recognizes the cleavage site between the two glycines in the C-terminal GG motif of ubiquitin. The same GG motif is found in exactly the same position in DWNN (residues 78 and 79) as it is in ubiquitin-like domains (Yamada *et al.* 2012). Interestingly, DWNN is expressed in vertebrates both as a single domain protein of 13 kDa, known as isoform 3, and as the N-terminal domain of the full length RBBP6 isoforms 1

and 2. In addition to the 81-residue DWNN domain, the 118-residue isoform 3 also contains a C-terminal tail, which is not found in the full-length protein. In humans, the sequence encoding the short tail is poorly conserved across species and unstructured, and is highly susceptible to proteolysis when expressed recombinantly in bacteria. The domain is stable without the tail and its structure was determined using nuclear magnetic resonance spectroscopy (Pugh *et al*. 2006).

Ubiquitination could be critical as the 3-end processing complex proceeds through a cycle of assembly, cleavage, poly(A) addition, and release from the mature mRNA. Otherwise, ubiquitin-mediated degradation could reduce the level of an inhibitor of processing or help maintain appropriate stoichiometry of the subunits that make up the processing complex. When ubistatin A (an inhibitor that binds near the hydrophobic patch on the surface of ubiquitin) interacts with ubiquitin-binding domains (UBDs) in an *in vitro* process, it blocks the interaction of ubiquitinated proteins with other proteins. The poly(A) addition, 3' -end processing and mRNA splicing *in vitro* was inhibited however, specific to protein having longer U-rich tracts flanking the cleavage site, RNA containing the CYC1 poly(A) site not the UA-rich efficiency element RNA containing the GAL7 site. When the proteasomal inhibitor MG132 was added in processing *in vitro*, it affected poly-adenylation suggesting that active protein degradation contributes directly to efficient processing *in vitro* (Lee and Moore 2014).

1.3 The role of RBBP6 in ubiquitination
1.3.1 The ubiquitin proteasome system
Ubiquitination is a post-translation modification that is involved in the control of activity and function of cellular proteins. It is one of the most important post-translation modifications, affecting the fate of proteins with a variety of outcomes, including proteasomal degradation, endosomal sorting, endocytosis, and DNA repair. The 8.5 kDa ubiquitin moiety is transferred to the target protein where it affects the target protein structure, activity, stability, localization, or interaction. Hence, ubiquitination orchestrates the regulation of a number of cellular processes such as membrane trafficking, signal transduction, cell division, apoptosis, and immune response (Wilkinson *et al.* 2005; Kulathu and Komander 2012).

Ubiquitination occurs when an ubiquitin moiety is covalently attached primarily to lysine residues, but less commonly to cysteine, threonine, or tyrosine residues, of the target protein (McDowell and Philpott 2013). Proteins are conjugated with ubiquitin via sequential action of enzymatic cascade involving E1, E2 and E3 enzymes. The ubiquitin-activating E1 activates ubiquitin through the formation of a high-energy thioester bond between the ubiquitin C-terminal glycine and the active cysteine in the E1, in the presence of adenosine triphosphate (ATP). Once activated, ubiquitin is transferred from the cysteine residue of E1 to a cysteine on the ubiquitin-conjugating E2 enzyme. Finally, the ubiquitin-conjugating E3 ligase forms a complex with the E2 conjugating enzyme to facilitate the transfer of ubiquitin to a lysine on the target protein where an isopeptide bond is formed between the backbone carboxyl group of the glycine and the side-chain amino group of the lysine (see Figure 1.2) (Pickart and Eddins 2004; Dye and Schulman 2007).

There are two isoforms activating E1 enzymes in human cells, and there are about 40 conjugating E2 enzymes. Moreover, there are thousands of ubiquitin E3 ligases because they are specific for the target substrate and there are many different proteins to be ubiquitinated (Semple *et al.* 2003). There are two classes of ubiquitin E3 ligase, those containing the homologous to E6-AP C-terminus (HECT) domain and those containing the really interesting new gene (RING) or the U-box domain (Deshaies and Joazeiro 2009). With HECT E3s become covalently attached to the Ub before being transferred to the substrate. Catalytic cysteine forms a thioester linkage with the C-terminus of Ub, identical to the E2-Ub linkage. The RING/U-box E3s, the RING finger is characterised by the presence of two zinc ions with a conserved pattern of eight cysteine or histidine residues in a "cross-braced" structure and U-boxes have identical structures, but do not bind any zinc ions and do not have the conserved Cys/His residues. In contrast to the HECT E3s, the RING-containing ligases facilitate the transfer of ubiquitin from the E2 to the substrate without any direct contact with ubiquitin (see Figure 1.2) (Dye and Schulman 2007, Metzger *et al*. 2014).
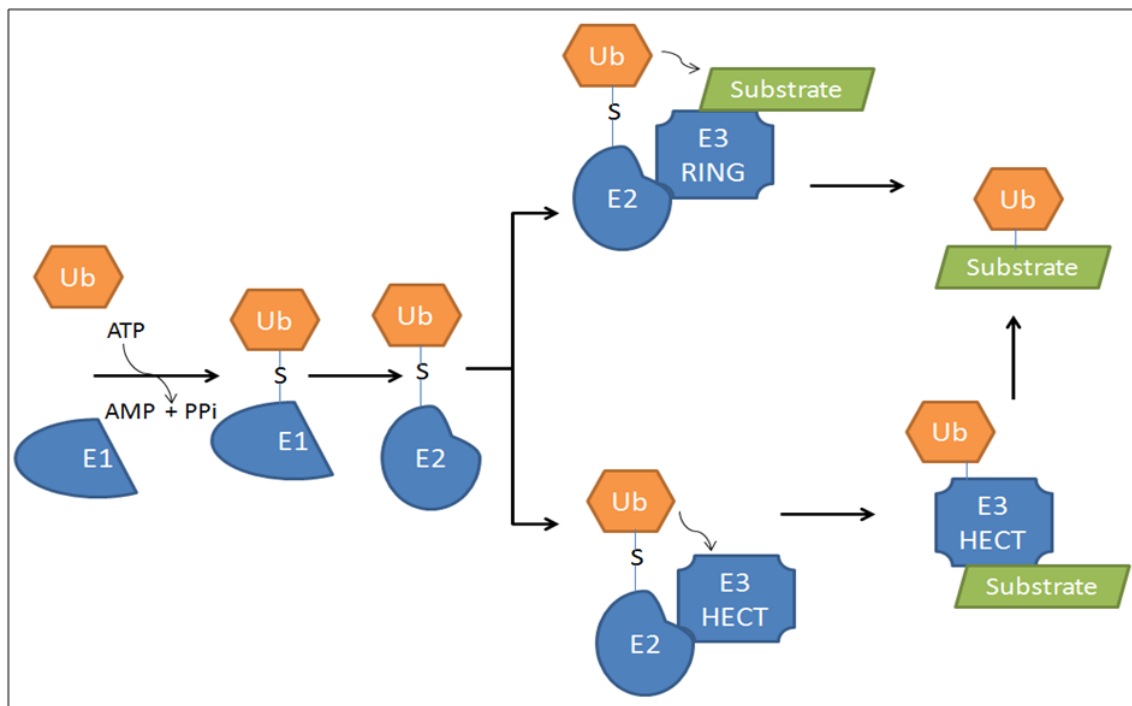
Figure 1.2: Schematic representation of ubiquitination mechanism. A cascade of enzymes is required to ubiquitinate substrate via sequential action. These enzymes include the activating E1 enzyme, conjugating E2 enzyme and E3 ligase. The two classes of E3 ligase, the RING and HECT are represented. HECT E3 ligases, directly contact ubiquitin before it is transferred to the substrate, while RING E3 ligases directly transfer ubiquitin to substrate, without any contact with ubiquitin molecule (Woelk *et al*. 2007).

1.3.2 Classification of the RING domain

RING-type or U-box domains are found in many different structural contexts. While many exist as monomers, a notable feature of RING-type or U-box E3s is their tendency to form homo-dimers and hetero-dimers. Dimerisation is of physiological significance because mutations on amino acids that disrupt dimer formation abolish E3 ligase activity. Although homo-dimer formation is common, many RING domains including cIAP, RNF4, BIRC7, Ring1b,etc, can also form hetero-dimers, in some cases preferentially, with an inactive RING partner such as BRCA1-BARD1, MDM2-MDMX (or HDMX/HDM4 in human), and RING1B–Bmi1 (Metzger *et al*. 2014). The inability of mutated RING fingers to promote ubiquitin transfer suggests that dimerisation of RING finger is vital to enhance the local concentration of E2 enzymes and to promote catalytic processing (Yin *et al*. 2009, Liew *et al* 2010).

The cysteine-rich region of RBBP6 between residues 249-335 has been classified as both the RING finger and the U-box, due to eight conserved cysteine and the two bound zinc ions and conserved pattern of hydrophobic residues, respectively (Aravind and Koonin 2000). The U-

boxes are considered the hallmark of E4 ligase, which facilitates the formation of ubiquitin chain during ubiquitination (Cyr *et al.* 2002). This nature stabilizes the structure of protein, for example, the presence of the zinc ion increases thermal and conformational stability of domains. Additionally, some RING fingers have been shown to be a homo-dimer, for example, MDM2 RING finger, and this nature has been shown to be pivotal in ubiquitination (Nikolay *et al*. 2004). Like the MDM2 RING finger, the structure of the RING finger from RBBP6 has previously been solved using Nuclear Magnetic Resonance spectroscopy (NMR) and shown to homo-dimerize along the same interface found in many RING fingers (see Figure 1.3).
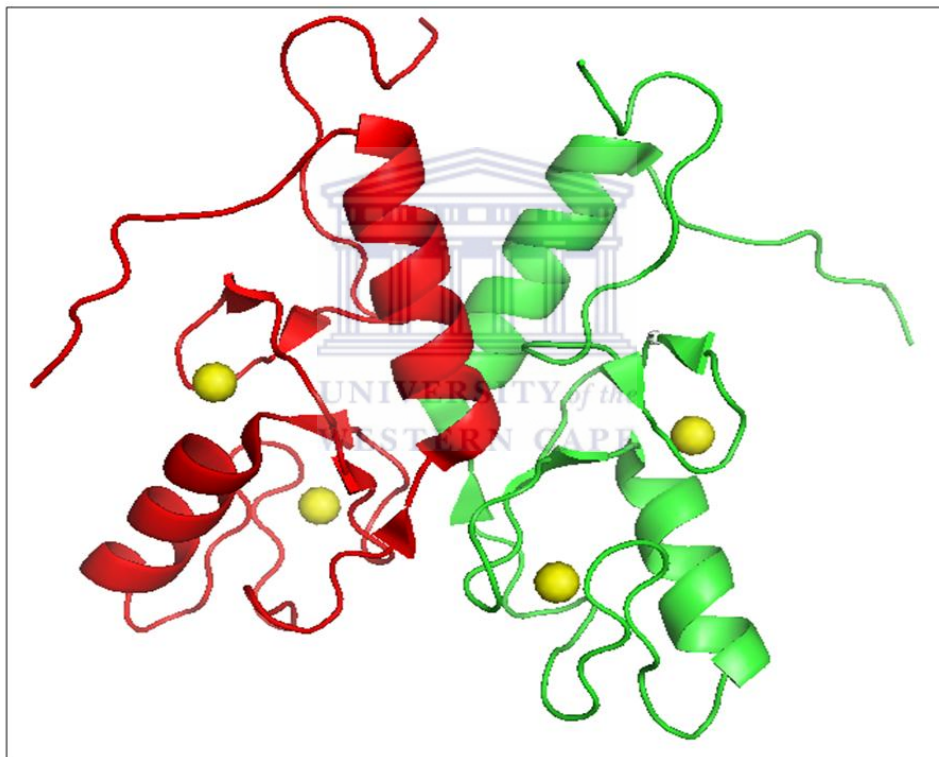
Figure 1.3: Cartoon secondary structure of the RBBP6 RING finger homo-dimer. Subunits of RBBP6 RING finger are shown in red and green, stabilized by the zinc ions in yellow spheres (Kappo *et al.* 2012).

RING fingers can be classified according to coordination of the zinc ion by cysteine (C) and histidine (H) residues; C3HC4 being the most common classification, although some classification such as C3HHC3 exist (Stone *et al*. 2005). Kappo and colleagues have shown that RBBP6 RING finger consists of eight conserved cysteine residues that coordinate the two zinc ions in a cross-braced fashion. This means that one of the zinc ions is coordinated

by the first and third cysteine residues and the other ion by the second and fourth cysteine residues. The Cys^{259}, Cys^{262}, Cys^{280}, and Cys^{283} are clustered and oriented to coordinate one Zn^{2+} ion. Similarly, Cys^{274}, Cys^{275}, Cys^{296}, and Cys^{299} are in proximity for another Zn^{2+} ion (see Figure 1.4). As the result, the RBBP6 RING is classified as C4C4 RING finger (Kappo *et al.* 2012).
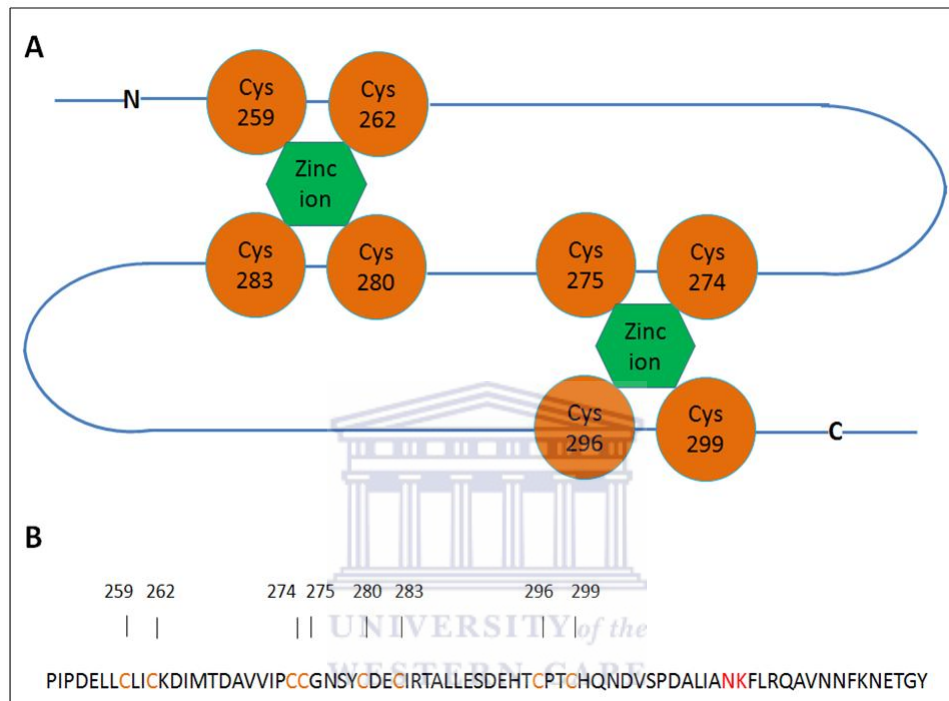
Figure 1.4: Cysteine residues involved in coordination of zinc ions in the RBBP6 RING finger. (**A**) Schematic representation of the RING finger domain indicating the 'cross-brace' topology for zinc ion coordination. (**B**) The sequence of the RING finger showing cysteine residues in orange and the residues, asparagine (N312) and lysine (K313) forming part of the homo-dimerization interface of the homo-dimer.

Dimerisation and oligomerisation can confer several different structural and functional advantages to proteins, including improved stability and activity. However, unwanted oligomerisations of proteins also lead to the formation of pathogenic structures (Marianayagam *et al.* 2004). The homo-dimeric RING E3s both RINGs have the intrinsic capacity to interact functionally with E2s, however, this appears not to be the case for some hetero-dimeric RINGs. MDM2 can homo-dimerize and is active, MDMX has little tendency to form a homo-dimer and it does not possess E3 ligase catalytic activity. However, the hetero-dimer formation of the RING domains of both MDM2 and MDMX is critical to retain the level of p53. The hetero-dimer formation of MDM2 and MDMX is important, as it enhances

the stability and activation of MDM2 during the inhibitory process of p53 (Tanimura *et al*. 1999; Okamoto *et al*. 2005; LeBron *et al*. 2006; Cheng *et al*. 2011). In BRCA1-BARD1, BRCA1 functions with E2, while its partners BARD1 serve to enhance activity, potentially interact with substrates and stabilize the complex (Hashizume *et al*. 2001).

1.3.3 Functional processes of ubiquitination

There are different ways in which post-translational modification by ubiquitin occurs. In mono-ubiquitination a single ubiquitin moiety attaches to a lysine residue of the target protein and orchestrates endocytosis, endosomal sorting, histone regulation, and DNA repair, virus budding and nuclear export. Multiple mono-ubiquitination is the transfer of a single ubiquitin moiety to several lysine residues of the target protein; this modification is involved in receptor internalization and endocytosis (Garcin *et al*. 2002, Oqawa *et al*. 2005, Gatza *et al*. 2007). Poly-ubiquitination occurs when a lysine residue on ubiquitin itself serves as acceptor of another ubiquitin moiety, thus forming a chain of ubiquitins. In many cases, it has been found that the same internal lysine is used predominantly in a poly-ubiquitin chain, allowing them to be classified as lysine48-linked chains or lysine63-linked chains. A chain of four or more ubiquitin monomers attached by linkages involving lysine48 (a so-called lysine48-linked poly-ubiquitin chain) promotes recruitment of the substrate to the 26S proteasome and its subsequent degradation. Lysine63-linked poly-ubiquitin chains can act as a signal for DNA repair, activation of transcription factors, endocytosis and activation of protein kinases (Hicke 2001; Weissman 2001; Hoppe 2005, Nathan *et al*. 2013).

The proteasome system orchestrates the quality of protein by degradation of damaged or mis-folded proteins (Brodsky and McCracken 1999; Davies 2001; Goldberg 2003). Proteins tagged with lysine48-linked poly-ubiquitin chain are degraded by the 26S proteasome in the presence of ATP, which degrades cytosolic proteins in eukaryotes (Chandu and Nandi 2004). The 26S proteasome consists of the 20S proteasome, which harbours the proteolytic site, and two 19S regulators. The 20S takes the form of a barrel made up of four rings of seven subunits each. The subunits fall into two types, α and β, giving a $\alpha_7\beta_7\beta_7\alpha_7$ configuration. The proteolytic active sites are located on β-subunits 1, 2 and 5, which have chymotryptic (cleaves after hydrophobic side-chains), tryptic (cleaves after positively charged side chains) and post-glutamyl (cleaves after negatively charged side-chains) respectively. Among the

three types of activity, the proteasome is capable of cleaving any polypeptide chain into very small peptides. The 19S regulator takes the form of a cap, which fits on one or both ends of the 20S subunit and regulates access in an ATP-dependent manner. The base of the 19S particle takes the form of a seven-fold ring of subunits with ATPase activity (see Figure 1.5) (Pickart and Cohen 2004; Nandi *et al*. 2006). Although the details are still to be worked out, it seems that, an interface on the 19S recognises and binds to lysine48-linked poly-ubiquitin chains, facilitating recruitment and unfolding of substrate proteins, resulting in the substrate being fed into the 20S barrel and degraded (Thrower *et al*. 2000, Belzile *et al*. 2010).
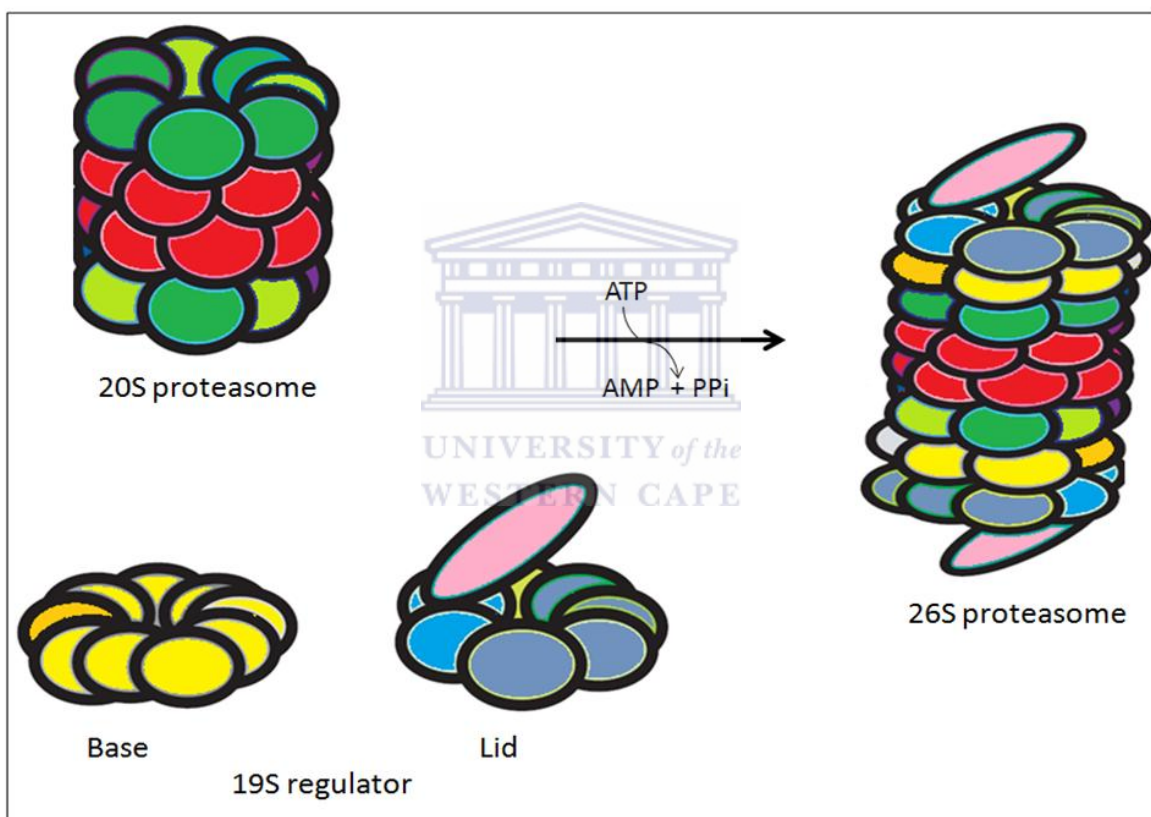
Figure 1.5: The formation of a 2000 kDa 26S proteasome. This system is formed by combination 700 kDa 20S proteasome and 19S regulator in the presence of ATP (Nandi *et al.* 2006).

MG132 (carbobenzoxy-Leu-Leu-leucinal) is a peptide aldehyde, which effectively inhibits the proteolytic activity of the proteasome. Han and colleagues showed that MG132 inhibits the growth of HeLa cells via inducing the cell cycle arrest as well as triggering apoptosis (Han *et al*. 2009). Protein ubiquitination and degradation are used in anti-cancer therapy, for example, Hsp90 inhibitor is used as anti-tumours agents, which prevent or inhibit the formation or growth of tumours. This small inhibitor affects the ubiquitination and

degradation of receptor and non-receptor kinases, including Erb-B2, epidermal growth factor receptor, and Src family kinases (Messaoudi *et al*. 2008).

RBBP6 is a RING finger-containing protein. As discussed earlier, RING fingers are closely associated with E3 ubiquitin-ligases, where their function is to recruit the ubiquitin-bound E2. E3s typically also contain a substrate-binding domain, which simultaneously recruits the substrate, leading to transfer of ubiquitin from the E2 to the substrate. For example, C-terminus of Hsp70 (CHIP) has a TPR-repeat domain at the N-terminus, which recruits substrates (Ballinger *et al*. 1999). Many E3 ligases have been shown to be able to ubiquitinate themselves (a process known as auto-ubiquitination). In many cases, this is likely to play a role in auto-regulation of the E3; however, auto-ubiquitination activity is often used as a proxy for substrate ubiquitination activity, especially in *in vitro* studies, where the absence of a separate substrate greatly simplifies the assay. The BCA2 protein, a RING-type E3 ubiquitin ligase is over-expressed in more than 50% of invasive breast cancers compared with normal tissues. It increases the proliferation of NIH3T3 fibroblasts, whereas siRNA inhibits the growth of BCA2-expressing. In addition, it is able to ubiquitinate itself dependent on its RING domain. BCA2 auto-ubiquitination activity correlates with its stability. When mutations of both the BZF domain cysteines and COOH-terminal lysines (K232R/K260R) located within and nearby the RING domain resulted in decreased amounts of BCA2 protein relative to wild-type protein in HEK293T cells. BCA2 RING is also required for BCA2 auto-ubiquitination and poly-ubiquitination is likely to be dependent on the two NH2- terminal lysines (Amemiya *et al*. 2008).

RBBP6 plays a role in ubiquitination of Y-Box Binding Protein 1 (YB-1) and zBTN38 (Chibi *et al*. 2008, Miotto *et al*. 2014). Y-box binding protein (YB-1) contains a "cold shock" domain (CSD) conserved in nucleic acid-binding proteins. It is a transcription factor and a translational regulator (Kohno *et al*. 2003). YB-1 has been described as an mRNA chaperone. YB-1 is also a cellular stress response factor that prevents the early onset of senescence in cultured cells *in vitro*. This was suggested after the requirements of YB-1 for the normal late embryonic development and survival of mice. YB-1 was reported to be ubiquitinated by the Skp-1/Cul1/F-Box (SCF) E3-ubiquitin ligase complex. F-Box protein, FBX33 belongs to an SCF E3-ubiquitin ligase that targets YB-1 for ubiquitination and degradation by the proteasome.

FBX33 is part of a SCF complex demonstrated after immunoprecipitated complexes revealed that FBX33 co-precipitated conserved SCF components Skp1, Cul1, and Rbx/Roc1. Hence, FBX33 binds to the CSD of YB1 and recruits the Skp-1/Cul1 to YB-1 (Lutz *et al*. 2006)

Using a yeast 2-hybrid assay with the RING finger from RBBP6 as bait, Chibi and co-workers identified the C-terminal 62 amino acids of YB-1 as an interaction partner of RBBP6 (Chibi *et al*. 2008). Overexpression of the RING finger in mammalian cells led to dose-dependent suppression of cellular YB-1 in a proteasome-dependent manner, suggesting that YB-1 was being ubiquitinated by RBBP6, leading to its destruction in the proteasome. In the same study the RING finger was shown to interact with the transcriptional repressor protein zBTB38 (Chibi et a 2008). In a subsequent study, RBBP6 was shown to ubiquitinate and destabilize zBTB38 protein, and to prevent DNA damage (Miotto *et al.* 2014). Knockdown of RBBP6 led to a decrease in ubiquitinated zBTB38 in cells and over-expression of RBBP6 to an increase in ubiquitinated zBTB38. Knockdown of RBBP6 represses MCM10 at the protein and mRNA levels and MCM10 is re-expressed in response to the knockdown of zBTB38. MCM10 is required for DNA replication in eukaryotes. RBBP6/zBTB38/MCM10 is critical for genome stability in mammalian cells (Miotto *et al*. 2014).
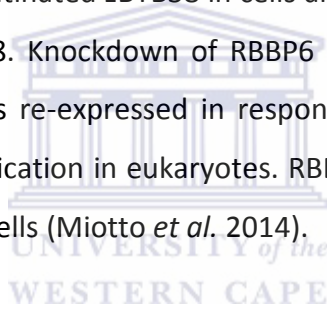
1.4 The role of RBBP6 in cancer

Cancer is an abnormal growth of cells caused by disregulation of cell proliferation and cell death. Ultimately, this can evolve into a population of cells that can invade tissues and metastasize to distant sites causing significant morbidity and, if untreated, mortality of the host. Researchers have demonstrated that over-expression of receptors and growth factors, oncogene activations, and inactivation of tumor suppressor genes are the source causes for the development of an aggressive and resistant cancer phenotype (Aggarwal *et al*. 2014). The architecture of tissues is highly regulated and there is extensive intracellular communication conducted primarily by mitogens and communicated into the cell by trans-membrane signalling pathways (Dhillon *et al*. 2007). For example, the p53 pathway responds to stresses that can disrupt the fidelity of DNA replication and cell division. A stress signal is transmitted to the p53 by post-translational modifications, which activate p53 as a transcription factor that initiates a program of cell cycle arrest, cellular senescence, or apoptosis. The transcriptional network of p53-responsive genes produces proteins that

interact with a large number of other signal transduction pathways in the cell and a number of positive and negative auto-regulatory feedback loops act upon the p53 response (Vogelstein *et al*. 2000, Lowe and Sherr 2003, Harris and Levine 2005).

A number of studies have found that RBBP6 is up-regulated in cancers. RBBP6 was found to be an independent prognostic factor for stem cells in gastric cancer. RBBP6 was one of eight genes found to be up-regulated in the side population (SP) cells, a sub-population of gastric cancer cells, which serve as a model for stem cells, relative to its levels in respective parent cell lines. Knockdown of RBBP6 with siRNA led to a significant decrease in the invasion and migration activity of SP cells, which established RBBP6 as a major marker for metastasis in gastric cancer (Morisaki *et al*. 2014).

In subsequent investigations, RBBP6 was found to significantly correlate with tumour progression in oesophageal cancer and cervical cancer. Up-regulation of RBBP6 was found in oesophageal cancer cells, whereby it correlates with poor clinical progression of oesophageal cancer (Yoshitake *et al*. 2004). The level of p53 in normal unstressed cells is low due to proteasomal degradation promoted by E3 ligase activity. In stressed cells, the level of p53 is in abundance, due to disruption of its degradation. In colon cancer, up-regulation of RBBP6 by mutant TP53 protein has been associated with a poor survival rate (Chen *et al*. 2013). The knockdown of RBBP6 with siRNA led to p53 gene expression involved in cell death pathways and apoptosis, hence, reduction of cell growth compared to the control sample. Silencing RBBP6 may therefore be a novel strategy to promote camptothecin-induced apoptosis in breast cancer cell (Moela *et al*. 2014). In conclusion, RBBP6 is a promising prognostic biomarker and a therapeutic target for variety of cancer.

1.5 Possible models for involvement of RBBP6 in regulation of p53
Studies of p53 functions have revealed that its regulation is crucial in understanding the defence mechanisms against cancer. It functions as a transcription factor for a number of genes - critical for cell cycle arrest, apoptosis, and senescence, and exhibit DNA binding activity. p53 is found to be deleted, mutated, or mis-regulated in the majority of cancers (Hainaut *et al.* 1997; Levine 1997). In normal unstressed cells, p53 is unstable and present at low levels to allow normal growth. Its levels increase rapidly in response to a variety of

genotoxic stresses, including X-rays, ultraviolet (UV) radiation and certain chemotherapeutic agents that damage DNA. Up-regulation of p53 induces the expression of a cohort of genes, including MDM2, cyclin G, GADD45, WAF1/p21/CIP1 and Bax, each regulating different aspects of cell growth arrest and apoptosis (Gottlieb and Oren 1998).

MDM2 is a transcriptional target of p53, creating a p53-MDM2 negative feedback loop which keeps cellular levels of both proteins low (Li *et al*. 2003, Hunziker *et al*. 2010). In contrast, in human cancer cells that carry mutant p53 alleles, there is excess p53 concentration. When mutated p53 loses its power as a transcription factor, it is unable to induce MDM2, through which it escapes the degradation process. Thus, human cancer cells often contain high concentrations of non-functional p53. MDM2 binding to p53 conceals its transactivation domain, thereby inhibiting p53-dependent effects on cell cycle inhibition and apoptosis (Barak *et al*. 1993, Harms and Chen 2006).

The tumour suppressor protein p53 induces the expression of a cohort of genes - MDM2, cyclin G, GADD45, WAF1/p21/CIP1 and Bax - critical for cell cycle arrest and apoptosis in response to stress to maintain the integrity of the genome through transcription-dependent and –independent mechanisms. RBBP6 interacts with p53 whereby it suppresses the binding of p53 to DNA (Simons *et al*. 1997). RBBP6 also cooperates with MDM2 (denoted as HDM2 in human) in ubiquitinating p53 leading to proteasomal degradation of p53 (Li *et al*. 2007).

Alternatively, it could be that RBBP6 is acting as an E4 ligase to activate the poly-ubiquitination activity of MDM2, which on its own is only able to catalyse mono-ubiquitinates of p53. Otherwise, it could be that RBBP6 is hetero-dimerizing with MDM2 to poly-ubiquitinate p53. To answer that question we would have to determine whether the RING fingers of RBBP6 and MDM2 interact. RBBP6 possibly displaces MDMX from MDM2/MDMX. Alternatively, does RBBP6 suppress itself by auto-ubiquitinating itself? To answer that question we would have to measure the auto-ubiquitination of RBBP6, which has never been done.

1.6 Questions to be addressed in the thesis

Retinoblastoma Binding Protein 6 (RBBP6) is a RING finger-containing protein that plays a role in 3'-end poly-adenylation of mRNA transcripts as well as acting as an E3 ubiquitin ligase against a number of proteins involved in tumourigenesis, including p53. Many E3 ubiquitin ligases form homo-dimers and dimerisation is important for their activity; structural studies of the isolated RING finger of RBBP6 showed that it forms a weak homo-dimer (Kappo *et al*. 2006). Auto-ubiquitination of an isolated RING finger *in vitro* has been reported previously (Everett *et al*. 2010). As a means of understanding the structural functions of RBBP6, a number of questions need to be answered: do larger fragments of RBBP6 form stronger homo-dimers than the isolated RING finger and, if so, how strong is the dimerisation, and which residues are involved in the dimerisation? Does the DWNN domain contribute to the dimer interface? Does RBBP6 auto-ubiquitinate itself, and does this catalyse degradation in the proteasome that may explain the low levels of RBBP6 found in most cells? Does RBBP6 interact directly with MDM2 and, if so, where is the interface? Do they possibly form hetero-dimers through their RING finger domains like those of MDM2 and MDMX?

This thesis aims to address three of these questions: (1) Can we identify a larger N-terminal fragment of RBBP6 which forms a stronger homo-dimer than the isolated RING finger (2) can RBBP6 auto-ubiquitinate itself and, if so, is dimerisation crucial for this activity, and (3) does the RING finger domain of RBBP6 interact with the RING finger of MDM2?

Chapter 2: Materials and Methods

2.1 Materials and suppliers

40 % 37.5:1 Acrylamide: bis-acrylamide	Promega
Acetone	Merck
Agarose	Sigma
Ammonium persulphate	Merck
Ampicillin	Sigma
Antibodies	Santa Cruz Biotechnology
Bovine serum albumin	Roche
Bromophenol Blue	Merck
Casein	Sigma
Clarity™ Western ECL substrate	BioRAD
DNAse I	Sigma
EDTA-free protease inhibitor cocktail	Roche
Ethanol	Merck
Ethylene Diamine Tetra Acetic Acid (EDTA)	Merck
GeneJet Gel Purification kit	ThermoFisher Scientific
GenElute HP Plasmid Miniprep Kit	Sigma
Glacial acetic acid	Merck
Glycerol	Merck
Glycine	Merck
Glutathione agarose	Sigma
Hydrochloric acid (HCl)	Merck
Imidazole	Sigma
Isopropanol	Merck
Isopropylβ-D-1-thiogalactopyranoside (IPTG)	Sigma
Kanamycin sulphate	Sigma
Lysozyme	Roche
Luria Bertani broth	Merck
Magnesium chloride	Merck
Methanol	Merck

16

N, N, N', N'-Tetra methylethylene-diamine (TEMED)	Sigma
Nutrient agar	Merck
Potassium Acetate	Merck
Potassium Chloride	Merck
Protein molecular weight standard	Fermentas
EDTA-free protease inhibitor cocktail	Roche
ATP magnesium salt (Mg.ATP)	Sigma
Monopotassium phosphate	Merck
Reduced glutathione (GSH)	Sigma
Restriction enzymes	Fermentas
RNAse A	Roche
Sodium azide	Merck
Sodium chloride	Merck
Sodium phosphate	Merck
T4 ligase	Fermentas
Tris(hydroxymethyl)-amino-methane	Merck
Triton X-100	Merck
Tryptone	Merck
Tween-20	Merck
Nickel sepharose	Amersham Biosciences
Zinc sulphate	Merck

2.2 General stock solutions, buffers, and media

<u>10x Phosphate buffered saline (PBS):</u>

1.36 M NaCl, 0.027 M KCl, 0.1 M Na2HPO4-7H2O, 0.18 M KH2PO4, adjusted to pH 7.4 with HCl.

<u>10x SDS electrophoresis buffer:</u>

25 mM Tris, 0.1 % (m/v) SDS and 250 mM Glycine.

<u>10x TBE (Tris/Borate/EDTA):</u>

0.9 M Tris (pH 8.3), 0.89 M boric acid and 25 mM EDTA, stored at room temperature and diluted ten-fold for electrophoresis agarose gels.

<u>2x SDS-PAGE Gel Sample Buffer:</u>

20 % (w/v) SDS, 1.5 M Tris (pH 6.8), 15 % (v/v) glycerol and 1.8 % (w/v) bromophenol blue, store at room temperature. In addition, 10 % (v/v) β-mercaptoethanol was added to the buffer immediately prior to use and stored at -20 °C.

50x Tris-acetate (TAE) DNA Electrophoresis Buffer:

2 M Tris-HCl, 1 M acetic acid and 0.05 M EDTA in dH2O, and stored at room temperature.

Ammonium persulfate:

10 % (w/v) APS in dH2O, and stored at -20 °C.

Ampicillin:

100 mg/ml in deionised water, filter-sterilised and stored at -20 °C.

Binding Buffer (Protein purification):

1x PBS, 5 % (v/v) glycerol, and 1 mM DTT.

Chloramphenicol:

34 mg/ml solution in ethanol, filter-sterilised and stored at -20 °C.

Cleavage buffer:

50 mM Tris, pH 8.0, 20 mM NaCl, and 1 mM DTT.

Coomasie Blue Staining Solution:

0.25 % (w/v) Bromophenol Blue, 40 % (v/v) ethanol, and 10 % (v/v) acetic acid in dH2O.

Destaining solution:

40 % (v/v) ethanol, 10 % (v/v) acetic acid made up with dH2O.

Dithiothreitol (DTT):

1 M DTT in 10 mM sodium acetate (pH 5.2), filter-sterilised and stored at -20 °C.

Isopropyl β-D-1-thiogalactopyranosid (IPTG):

1 M IPTG in deionised water, filter-sterilised and stored at -20 °C.

Kanamycin:

30 mg/ml in distilled water, filter-sterilised and stored at -20 °C.

Luria Bertani Agar:

10 g/l tryptone, 5 g/l yeast extract, 5 g/l sodium chloride and 10 g/l agar in dH2O.

Luria Bertani Broth:

10 g/l tryptone, 5 g/l yeast extract, and 5 g/l sodium chloride in dH2O.

Lysis Buffer:

50 mM Tris, pH 8.0, 150 mM NaCl, 0.5 % (v/v) Triton X-100, 5 % (v/v) glycerol, 1 mM DTT,

100 μM ZnSO4, CompleteTM EDTA-free protease inhibitor cocktail, 50 μg/ml DNAse and 100

µg/ml lysozyme.

Mg.ATP:

0.1 M Mg.ATP in dH2O.

Nutrient agar:

31 g/l nutrient agar in distilled water.

PBS-T (Phosphate buffered saline-Tween-20):

1x PBS containing 0.1 % (v/v) Tween 20.

Separating Buffer:

1.5 M Tris-HCl, adjusted to pH 8.8 with HCl.

Sodium acetate:

2 M sodium acetate in deionised water, adjusted to pH 5.2 with diluted acetic acid.

Stacking Buffer:

0.5 M Tris-HCl, adjusted to pH 6.8 with HCl.

Transformation buffer 1 (Tfb1) buffer:

30 mM Potassium acetate, 50 mM MnCl2, 0.1 M KCl, 10mM CaCl2 and 15 % (v/v) glycerol.

Transformation buffer 2 (Tfb2) buffer:

9 mM MOPS, 50 mM CaCl2, 10 mM KCl and 15 % (v/v) glycerol.

Transfer Buffer:

25.9 M Glycine, 20.9 M Tris, and 779.9 M SDS in 20 % (v/v) ethanol and stored at -20 °C.

Tris-HCl Buffer:

1 M Tris-HCl, adjusted to pH 8.0 with HCl.

TYM:

20 % Tryptone, 0.5 % Yeast Extract, 0.1 M NaCl, 0.2 % (w/v) glucose, and 10 mM MgCl2.

Wash Buffer:

1x PBS and 1 mM DTT.

Zinc Sulphate:

0.1 M ZnSO4 in dH2O.

2.3 Antibodies used for immunoblotting

Anti-RBBP6-RING: rabbit polyclonal raised in the laboratory of Prof Dirk Bellstedt, Department of Biochemistry, University of Stellenbosch, against a recombinant fragment corresponding to residues 249-335 of full-length human RBBP6.

Ubiquitin antibody: rabbit polyclonal IgG with epitope corresponding to amino acid residues 1-76 representing full-length ubiquitin of human origin, Santa Cruz Biotechnology Inc (Santa Cruz, CA, USA); product code sc-9133

2.4. Expression plasmids
2.4.1 pGEX-6P-2
The pGEX vector was developed employing a gene encoding Glutathione S-transferase (GST) from the parasitic helminth *Schistosoma japonicum* (Smith and Johnson 1988). The 26 kDa GST moiety binds with high affinity to glutathione coupled to a Sepharose matrix. GST fusion protein can be applied in the study of protein-protein interactions via GST pull down assays (Singh and Asano, 2007).

The pGEX-6P-2 vector (GE Healthcare Life Sciences, Chalfont St Giles, UK) (see Figure 2.1 panel A) allows bacterial expression of target proteins attached to the C-terminus of the 26 kDa glutathione-S-transferase protein from *Schistosoma japonicum*. Expression is driven by a *tac* promoter which is induced by the synthetic lactose analogue Isopropyl β-D-1-thiogalactopyranoside (IPTG). It contains a multiple cloning site (MCS) (see Figure 2.1 panel B), to facilitate the un-directional cloning of DNA inserts. The 3C protease site - Leu-Glu-Val-Leu-Phe-Gln-Gly-Pro - between the GST-tag and the MCS allows the removal of GST from the fusion protein following expression. Removal of the GST tag leaves a residual five-residue sequence Gly-Pro-Leu-Gly-Ser attached to the N-terminus of the protein. The vector incorporates an ampicillin resistant gene, to allow bacterial resistance to the antibiotic (ampicillin)

2.4.2 pET-28a
Members of the pET family of expression vectors (Merck KGaA, Darmstadt, Germany) use a T7 promoter to reduce leaky expression in *Escherichia coli (E. Coli)* expression hosts since it is not recognised by host RNA polymerases. T7-specific polymerases are supplied from a T7 RNA polymerase gene incorporated into the chromosome of DE3 expression hosts, under control of a *lac* promoter. Addition of IPTG induces expression of the T7 RNA polymerase, which in turn, induces expression of the target gene. The pET-28a vector allows for the

optional addition of either N- or C-terminal 6His tags, dependent on the sites of incorporation of the target gene, as can be seen from the multiple cloning cassettes shown in Figure 2.2. The vector incorporates a kanamycin resistance gene to allow selection with kanamycin.

A

(4885) **BtgI**
(4777) **Bsu36I**
BfuAI - BspMI (62)
lac operator
EcoNI (268)
MscI (465)
BstBI (655)
SwaI (685)

(4327) **PluTI**
(4325) **SfoI**
(4324) **NarI***
(4323) **KasI**

tac promoter

GST

500

pGEX 5' Sequencing Primer (869 .. 891)
PasI (941)
BamHI (945)
EcoRI (955)
TspMI - XmaI (960)
SmaI (962)
SalI (965)
AccI (966)
PaeR7I - PspXI - TliI - XhoI (970)
EagI - NotI (976)
stop codons
PfoI (1052)
pGEX 3' Sequencing Primer (1035 .. 1057)
PflFI - Tth111I (1155)
BsaAI (1162)
ZraI (1259)
AatII (1261)

(4134) **EcoRV**
(4095) **BssHII**

(3865) **BstEII**

(3684) **MluI**

lacI

PreScission site

MCS

1000

AmpR promoter

AmpR

1500

pGEX-6P-2
4985 bp

UNIVERSITY of the
WESTERN CAPE

(3367) **BstAPI**
(3266) **PflMI**

lacIq promoter

ori

2000

3000
2500

PstI (1938)
BsaI (2114)
AhdI (2180)

(2659) **AlwNI**

B
pGEX-6P-2 (27-4598-01)
PreScission Protease

| Leu | Glu | Val | Leu | Phe | Gln↓ | Gly | Pro | Leu | Gly | Ser | Pro | Gly | Ile | Pro | Gly | Ser | Thr | Arg | Ala | Ala | Ala | Ser |
| CTG | GAA | GTT | CTG | TTC | CAG | GGG | CCC | CTG | GGA | TCC | CCA | GGA | ATT | CCC | GGG | TCG | ACT | CGA | GCG | GCC | GCA | TCG |

BamH I   EcoR I   Sma I   Sal I   Xho I   Not I

Figure 2.1: Restriction map and main features of the pGEX-6P-2 vector. (A) The pGEX-6p-2 vector is a 4985 bp C-terminal GST expression vector with a *tac* promoter, allowing induction of expression of the target protein using IPTG. (B) The multiple cloning site (MCS), into which the target cDNA is inserted, immediately following the 3C protease site. Proteolytic cleavage of the fusion protein takes place as indicated by the small arrow, leaving a number of residues attached to the beginning of the target protein. Figure generated using SnapGene Viewer snapgene.com.
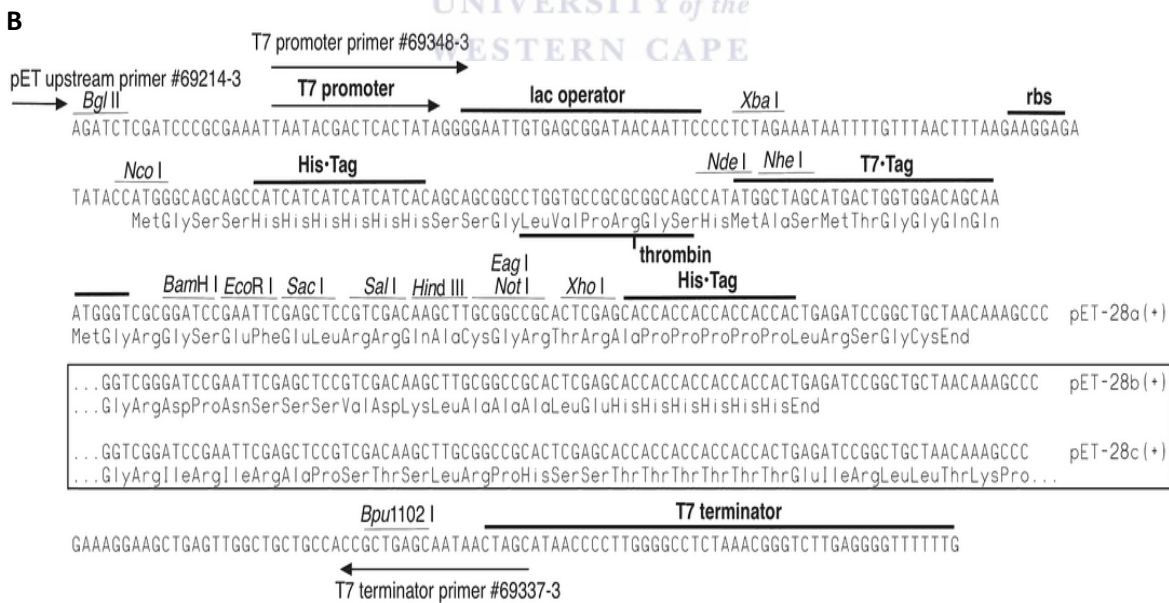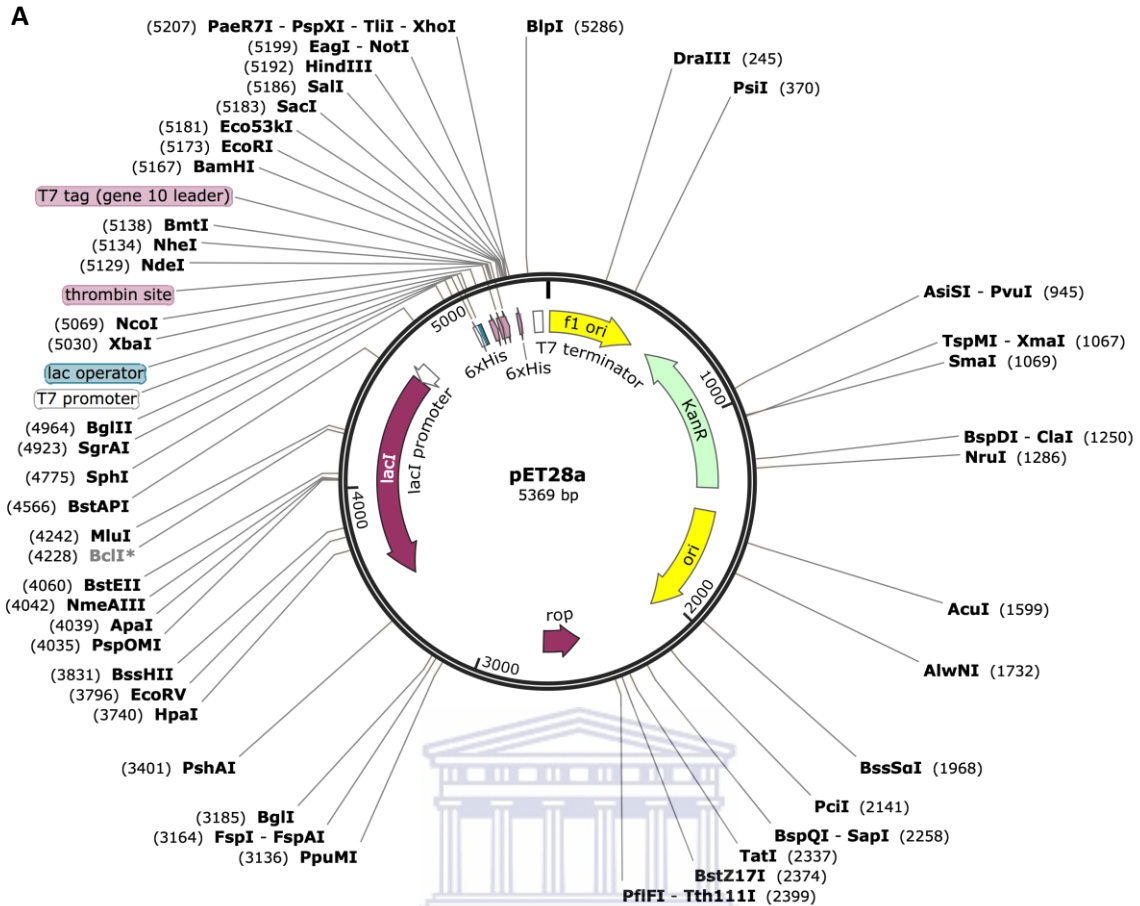
Figure 2.2: Restriction map and main features of the pET-28a vector. (A) The pET-28a vector is a 5369 bp expression vector allowing for incorporation of both N-terminal and C-terminal 6His-tags. The recombinant protein is expressed under the control of a T7 promoter, which is induced indirectly by IPTG in DE3 expression hosts. (B) The multiple cloning site (MCS) allows for the optional addition of both N- and C-terminal 6His-tags, dependent on the sites of insertion of the target gene. Figure generated using SnapGene Viewer snapgene.com.

2.5 Bacterial culture
2.5.1 Bacterial strains used
Escherichia coli strain DH5α: F$^-$ endA1 glnV44 thi-1 recA1 relA1 gyrA96 deoR nupG Φ80d_lacZ_ΔM15 Δ(_lacZYA-argF_)U169, hsdR17(r$_K^-$ m$_K^+$), λ−. This strain was used to produce plasmid DNA.

Escherichia coli strain XL10-Gold: endA1 glnV44 recA1 thi-1 gyrA96 relA1 lac Hte Δ(mcrA)183 Δ(mcrCB-hsdSMR-mrr)173 tet^R F'[proAB lacI^{q}ZΔM15 Tn10(Tet^R Amy Cm^R)]. This strain was used to produce plasmid DNA.

Escherichia coli strain BL21 (DE3) pLysS: F$^-$ ompT gal dcm lon hsdS$_B$(r$_B^-$ m$_B^-$) λ(DE3) pLysS(cm^R). This strain was used to express recombinant proteins. Since it is a DE3 strain, it is suitable for use with pET expression vectors.

Escherichia coli strain BL21-CodonPlus (DE3)-RIPL: B F$^-$ ompT hsdS(r$_B^-$m$_B$) dcm$^+$ Tetr gal λ(DE3) endA Hte [argUproLCam^r] [argU ileY leuW Strep/Spec^r]. This strain was used to express recombinant proteins. Since it is a DE3 strain, it is suitable for use with pET expression vectors. It incorporates additional copies of tRNA genes corresponding to codons abundant in mammalian genes but rare in bacterial genes, increasing the efficiency of expression of mammalian genes in bacteria.
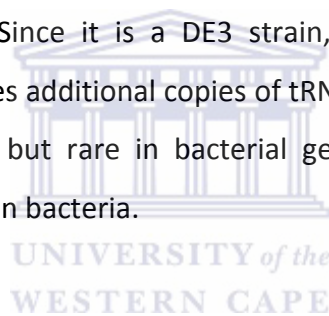
2.5.2 Antibiotic selection
E. coli cells were plated on nutrient agar containing either 100 µg/ml of ampicillin or 30 µg/ml of kanamycin (Kan) depending on the resistance of the plasmid. The same concentration of antibiotics was used to maintain selection during bacterial growth in liquid culture.

2.5.3 Preparation of competent _Escherichia coli_ cells for transformation
The desired strain of cells was streaked on a nutrient agar plate containing 10 mM MgSO$_4$ and incubated overnight at 37 °C. From the plate, a single colony was inoculated in a 20 ml of TYM broth, and incubated overnight at 37 °C with vigorous shaking. Then, 5 ml to 15 ml of the overnight culture was scaled up to 100 ml with TYM broth and incubated at 37 °C until the optical density at 550 nm (OD$_{550}$) of 0.2 was reached. Thereafter, a 100 ml culture was diluted to 400 ml with fresh TYM broth and cells were grown at 37 °C until OD$_{550}$ was between 0.4 and 0.6.

Subsequently, cells were rapidly chilled in ice water, with swirling, transferred into a 500 ml tube and bacterial culture was sedimented by centrifugation at 6000 rpm for 10 min, in a pre-cooled Beckman JA-10 rotor. The supernatant was discarded and the bacterial pellet was re-suspended in 50 to 250 ml ice cold transformation buffer 1 (Tfb1) and incubated on ice for 30 min. Cells were recovered by centrifuging at 6000 rpm for 10 min. The supernatant was discarded and a pellet was re-suspended in 30 ml ice-cold transformation buffer 2 (Tfb2). Subsequently, aliquots of 150 ml cells were prepared and directly incubated at - 80 °C.

2.5.4 Transformation of plasmid DNA into competent *Escherichia coli* cells

100 to 400 ng of plasmid DNA was added to pre-cooled 1.5 ml microfuge tube. Into the same tube, 50 µl of competent cells was added and mixed by gentle tapping and incubated on ice for 30 min. A control tube was set with competent cells but no plasmid DNA. Cells were transformed by heat shock at 42 °C for 45 seconds, and were then allowed to recover by incubating on ice for 5 min. Thereafter 500 µl of pre-warmed Luria Bertani broth (LB) was added and the bacterial culture was incubated at 37 °C in a shaking incubator for 60 min. Following incubation, 50 to 200 µl of transformed cells was plated on pre-warmed LB agar plates containing the appropriate antibiotic and incubated inverted for 16 hours at 37 °C.

2.6 Preparation and manipulation of plasmid DNA
2.6.1 Extraction of plasmid DNA

A single colony of the transformed cells was inoculated in 20 ml of LB containing the appropriate antibiotic and incubated for 16 hours at 37 °C with vigorous shaking. The bacterial culture was sedimented by centrifugation at 43000 rpm for 10 min, in a pre-cooled Heraeus Megafuge 1.0R (ThermoFisher Scientific, Waltham MA, USA). Then, the supernatant was discarded. The plasmid DNA was extracted using the Wizard®Plus SV Miniprep Kit (Promega Corporation, Madison WI, USA) according to manufacturer's instructions. The analysis of purity and quantification of the concentration of the plasmid DNA was determined using a NanoDrop ND-1000 Spectrophotometer (ThermoFisher Scientific, Waltham MA, USA).

2.6.2 Site directed mutagenesis

In vitro site-directed mutagenesis was carried out using the QuikChange[TM] Site Directed Mutagenesis Kit (Stratagene, San Diego CA, USA) according to the manufacturer's instructions. Synthesized oligonucleotides incorporating desired mutation were mixed with components in the reaction mixture (See Table 2.1). Conditions for thermal cycling were as follows:

Initial denaturation at 95 °C for 1 minute

Denaturation at 95 °C for 30 seconds

Annealing at 55 °C for 1 minute   10 cycles

Extension at 68 °C for 10 minutes

Table 2.1: PCR reaction mixture for site directed mutagenesis

Components of reaction mixture	Concentration/volume
10x Reaction Buffer	1x
dsDNA template	50 ng/µl
Oligonucleotide primer forward	125 ng/µl
Oligonucleotide primer reverse	125 ng/µl
30 µl dNTP mix	1 µl
2.5 U/µl *Pfu Turbo*[TM] DNA polymerase	2.5 U
Nuclease free H$_2$O	Add to final volume of 50 µl

PCR reaction products were kept on ice for 2 min to lower the temperature below 37 °C. To ensure that sufficient amplification occurred, 10 µl of the reaction product was electrophoresis in 1x TAE buffer on a 1 % (w/v) agarose gel. Afterwards, 1 µl of *Dpn* I enzyme (10 U/µl) was added to the reaction products and mixed thoroughly by gently pipetting the solution up and down. The reaction mixture was spun down and incubated at 37 °C for 1 hour to digest the non-mutated template DNA. The *Dpn* I-treated DNA was transformed into *E.coli* DH5α competent cells and the plasmid was isolated using GeneJet Plasmid Miniprep Kit (ThermoFisher Scientific, Waltham MA, USA) according to manufacturer's instructions. The introduced mutation was confirmed by direct DNA sequencing.

2.6.3 PCR amplification of target DNA

Oligonucleotide primers were designed with different restriction enzyme sites. The forward primer incorporated the *XhoI* restriction site while the reverse primer incorporated the *NcoI* restriction site. The complementary restriction enzyme sites were in the pET-28a expression vector. The target DNA was successfully amplified using Dream Taq DNA Polymerase (ThermoFisher Scientific, Waltham MA, USA), according to manufacturer's instructions. The PCR mixture, which consisted of components in Table 2.2, was mixed with oligonucleotide primers that incorporated the desired restriction site. In the final analysis, PCR amplified product was electrophoresis in 1x TAE buffer on 1 % (w/v) agarose gel. PCR thermal cycling conditions were as follows:

Initial denaturation at 95 °C for 3 minutes

Denaturation at 95 °C for 30 seconds

Annealing at 67 °C (Tm-5 °C) for 45 seconds

Extension at 72 °C for 30 seconds

Final extension at 72 °C for 10 minutes

30 cycles

Table 2.2: PCR reaction mixture for amplifying target DNA

Components of reaction mixture	Concentration/volume
10 X Dream Taq Buffer	1 X
dsDNA template	50 ng/µl
Oligonucleotide primer forward	1 µM
Oligonucleotide primer reverse	1 µM
10 mM dNTP mix	0.2 mM
5 U/µl Dream Taq DNA polymerase	1.5 U
Nuclease free H_2O	Add to final volume of 50 µl

2.6.4 Cloning of DNA fragment into the expression vector

FastDigest enzymes (ThermoFisher Scientific, Waltham MA, USA) were used to digest the ends of the PCR amplicon and to open up the cloning vector, using the quantities set out in Table 2.3. Digested fragments were separated from contaminating enzymes and

oligonucleotides on 1 % (w/v) agarose gels and the relevant bands excised using the GeneJet Gel Extraction kit (ThermoFisher Scientific, Waltham MA, USA)

Table 2.3: Restriction enzyme digestion of vector DNA and DNA insert

Components of reaction mixture	Concentration/Volume	
	Expression Vector	PCR product
10x FastDigest Buffer	1x	1x
DNA	1 µg	0.2 µg
20 µl FastDigest enzyme/s	1 µl	1 µl
Nuclease free water	Add to 20 µl	Add to 30 µl

The small size of the fragments released when the vector was doubly digested made it difficult to confirm that both enzymes were in fact digesting the vector efficiently. For that reason, single digests with both enzymes were also performed to act as positive controls for the enzymes.

Digested PCR fragments were ligated into digested plasmid using the quantities set out in Table 2.4. The ligation reaction mixture was incubated at 22 °C for one hour using T4 DNA ligase, whereafter it was inactivated by incubating it at 70 °C for 5 min. 5 µl of the ligation reaction mixture was then transformed into competent *E. coli* XL10-Gold cells, as described in Section 2.5.4. The digested vector without the DNA insert was transfected in parallel to serve as a negative control. Cells from the experimental and the control transformations were plated out and grown overnight at 37 °C on agar containing 100 µg/ml antibiotics, as described in section 2.5.2.

The following morning the numbers of colonies on the experimental (with insert) and the control (without insert) were counted and compared to determine whether there were significantly more on the experimental than the control plates. If there were, the cloning was deemed likely to have been successful. To confirm this conclusion, colonies from both experimental and control plates were picked using an autoclaved pipette tip and inoculated into 20 ml LB media containing the appropriate antibiotic and grown overnight at 37 °C.

Cells were sedimented by centrifuging using a Heraeus Megafuge 1.0R (ThermoFisher Scientific, Waltham MA, USA) for 15 min at 4300 rpm and plasmid DNA extracted using the GeneJet Plasmid Miniprep Kit (ThermoFisher Scientific, Waltham MA, USA). Double digestion using the restriction enzymes used in the cloning was carried out in order to release a fragment of the same size as the original PCR product. Positive clones were subjected to direct DNA sequencing; experimental sequence reads were compared against the expected sequences using the Blast2 server at the NCBI (http://blast.ncbi.nlm.nih.gov/Blast.cgi).

Table 2.4: Ligation reaction mixture of digested vector DNA and insert DNA

Components of reaction mixture	Concentration/Volume
Vector DNA	50 ng
Insert DNA	250 ng
10x T4 DNA Ligase Buffer	2 μl
T4 DNA Ligase	1 U
Nuclease free water	Add to 20 μl

2.7 Expression and extraction of recombinant protein

Single colonies of transformed *E. coli* cells were inoculated into 100 ml LB containing 100 μg/ml ampicillin (Amp) or 30 μg/ml kanamycin (Kan) and 34 ug/ml chloramphenicol, followed by incubation at 37 °C with vigorous shaking overnight. The next morning the 100 ml E. *coli* culture was scaled up to 1 L with 900 ml of LB containing the appropriate antibiotic and then incubated at 37 °C shaking until the optical density at 550 nm (OD$_{550}$) was between 0.4 and 0.6. Thereafter, protein expression was induced by the addition of IPTG to a final concentration between 0.5 - 1 mM and incubated overnight with shaking at a temperature between 25 °C and 30 °C. Cultures of RING finger-containing proteins were supplemented with 100 μM ZnSO$_4$ to provide the necessary zinc ions. In the morning bacterial cells were sedimented by centrifugation in a pre-cooled centrifuge at 6000 *g* for 15 min. Pellets were then re-suspended in lysis buffer and stored at -20 °C until required for extraction of exogenous protein.

2.8 Protein Purification

2.8.1 Cell lysis

Cell pellets were thawed on ice after which cells were lysed by sonication, which comprised of 5 cycles: 30 seconds pulse, 30 seconds on ice. After sonication, cell lysate was centrifuged at 4 °C at 4300 rpm for 30 min to clear the lysate. The initial purification of the target protein out of cell lysate was carried out using self-poured gravity-flow columns containing glutathione-conjugated agarose (Sigma, St. Louis, MO, USA) in the case of GST-tagged proteins, or immobilised nickel sepharose (GE Healthcare Life Sciences, Chalfont St Giles, UK).

Purification was carried out off-column so that the media could be periodically removed from the column, and thoroughly cleaned using 2 M NaCl, to enable it to be re-used multiple times. Columns were prepared by pouring 5 ml of the appropriate slurry into 20 ml disposable columns (BioRAD, Hercules CA, USA) and equilibrating with 5 column volume (CV) wash phosphate buffered saline. The clarified lysate was added into the column and the flow through was collected. The column was then washed with 3 CV of the Wash Buffer containing 40 mM imidazole in the case of the nickel sepharose column to reduce non-specific binding. The protein of interest was then eluted from the column with Wash Buffer containing 20 mM reduced glutathione for glutathione agarose column or 500 mM imidazole for nickel sepharose column. Following elution columns were washed with 2 M NaCl containing 0.1 % of NaN_3 and stored in 4 °C for re-use.

2.8.2 Removal of GST

Depending on the application, either GST was left attached to the target protein or proteolytically removed using 3C protease. The cleaved target protein was then separated from GST by a second round of glutathione affinity purification, following dialysis to remove free glutathione remaining from the first round of purification; the target protein was recovered in the flow through with the GST, un-cleaved GST-target, and GST-3C being retained by the column and subsequently eluted as described previously.

In practice, the cleavage and removal of free glutathione were achieved successfully in one step. An un-cleaved fusion protein was transferred to SnakeSkin® Pleated Dialysis Tubing

(MWCO 3500 Da) (ThermoFisher Scientific, Waltham MA, USA), the bag was placed in 1 litre of Cleavage buffer and dialysed overnight at 4 °C with stirring.

2.9 Size exclusion chromatography

Residual GST and other contaminants were removed using size exclusion chromatography. The sample was concentrated into 5 ml and loaded onto a 120 ml Superdex 75 16/600 column (GE Healthcare Life Sciences, Chalfont St Giles, UK), operated on an ÄKTA FPLC chromatography platform (GE Healthcare Life Sciences, Chalfont St Giles, UK). Eluting proteins were collected in 2 ml fractions using an automated fraction collector. The same column was used to estimate the molecular weight of proteins. Within a range of molecular weights of the proteins determined by the sizes of particles making up the matrix, a linear relationship is expected between the logarithm of the molecular weight (MW) and the elution volume (Ve). In the case of the Superdex 75 matrix, linearity is only expected over the range 10 – 75 kDa, as can be seen from Figure 2.3. This phenomenon can be used to give reasonably good estimates of the effective molecular weight of a protein complex by comparing it with a standard curve generated using proteins of known molecular weight.
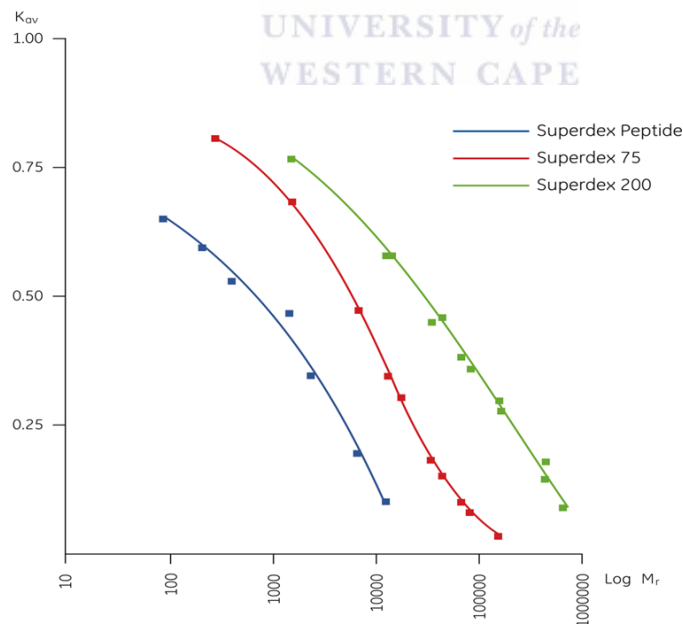
Figure 2.3: Selectivity curves for Superdex SEC medium. The red solid line, which corresponds to Superdex 75, is roughly linear over the region 10000 – 75000 Da and can therefore be used to estimate effective molecular weights only over that range (GE Healthcare Life Sciences).

2.10 Preparation of self-cast gels for sodium dodecyl sulfate polyacrylamide gel electrophoresis (SDS-PAGE)

Purified fractions were analysed by SDS-PAGE using the BioRAD Mini-Protean system (BioRAD, Hercules CA, USA). Gels were self-poured using Laemmli's method (Laemmli, 1970), consisting of a 4 % (w/v) stacking gel on top of a 16 % (w/v) resolving. Exact quantities are set out in Table 2.5

Table 2.5: Preparation of self-cast gels for SDS-PAGE

Components	16 % Resolving gel solution	4 % Stacking Gel solution
Buffer	2.63 ml (1.5 M Tris-HCl)	1.25 ml (0.5 M Tris-HCl)
40 % (v/v) acrylamide: bis-acrylamide	8 ml	0.5 ml
10 % (w/v) SDS	105 µl	50 µl
10 % (w/v) APS	50 µl	25 µl
dH$_2$O	3.2 ml	4 ml
TEMED	10 µl	7.5 µl

Proteins were prepared for SDS-PAGE by mixing 20 µl sample with equal volume of 2x SDS-PAGE gel sample buffer, followed by incubation at 95 °C for 5 min. Samples were centrifuged for 2-5 min to pellet insoluble materials and then 10 µl to 15 µl were loaded into each well. Proteins were separated at a constant voltage of 150 V per gel. Following electrophoresis gels were removed from the plates and incubated in Coomassie Staining Solution for approximately 30 min with gentle rocking on an orbital shaker. Thereafter the gel was rinsed with water, and then incubated in a de-staining solution until the background was clear.

2.11 *In vitro* auto-ubiquitination and proteasomal degradation of RBBP6-RING

Bacterially expressed and purified E2, E1, and ubiquitin were kindly supplied by co-workers in the laboratory, Ms Lauren Jooste and Ms Tephney Hutchinson. Purified RBBP6-RING concentrations were estimated by measuring the absorbance at 280 nm using a NanoDrop ND-1000 Spectrophotometer (ThermoFisher Scientific, Waltham MA, USA) on the assumption that a concentration of 1 mg/ml has an absorbance of 1 unit. The final volume of the reaction was scaled up to 50 ml with PBS after the addition of the required

components for auto-ubiquitination. In addition to E1, E2 and ubiquitin, 4 mM Mg-ATP was added to the reaction mixture. The experimental reaction mixture consisted of all the components. After 2 hours 1 mM of purified proteasome (kindly purified from Hela cells by Ms Tephney Hutchinson) was added and samples were incubated overnight.

2.12 *In vitro* GST pull down assays

GST fusion proteins GST-RBBP6 and GST-MDM2 were expressed in bacteria and purified on glutathione sepharose to serve as bait. MDM2-6His was expressed in bacteria and purified on nickel column to serve as bait. GST was cleaved off fusion RBBP6 and purified to serve as prey. 0.5 mg/ml GST fusion protein, 0.12 mg/ml of prey and 20 μl glutathione agarose (20 % (m/v) slurry made using Binding Buffer) was incubated overnight mixing at 4 °C. The mixture was centrifuged at 1700 rpm for 2 min in a micro-centrifuge to pellet the beads and the supernatant was transferred into a fresh tube. The beads were then washed by re-suspending in 1 ml 1x PBS containing 2 mM DTT, followed by centrifugation at 1700 rpm for 2 min, this step was repeated five times. Finally, beads were re-suspended in 20 μl of 2x SDS-PAGE gel sample buffer. Samples were then boiled at 95 °C for 10 min, followed by centrifugation for 2 min. 12 μl of the sample was separated on SDS-PAGE and used for Western blot analysis.
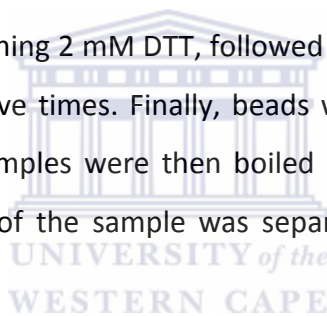
2.13 Immunodetection of proteins (Western blotting)

Protein samples were separated using SDS-PAGE, as described in Section 2.8.5. A piece of 0.2 μm, Immun-Blot® PVDF membrane (BioRAD, Hercules CA, USA) was cut to the same size as the gel and activated in 20 ml 2-propanol. Six pieces of MN218B blotting paper (Macherey Nagel, Düren, Germany) were cut to the same size. Both the membrane and the filter papers were equilibrated in Transfer Buffer and then assembled into the blotting cassette consisting of this order: three filter papers membrane, gel, and three filter papers. The cassette was loaded into the tray of the Trans-Blot® Turbo™Blotting System (BioRAD, Hercules CA, USA) and transfer performed for 20 min. Following the transfer, the membrane was blocked for 1 hour with 1 % (w/v) casein in PBS-T and then incubated for 1 hour with the appropriate primary antibodies. Following 3 x 10-min washes with PBS-T, the membrane was incubated with the appropriate HRP-conjugated secondary antibodies for 1 hour, followed by 3 x 10-min washes with PBS-T. The membrane was incubated with Clarity™

Western ECL Substrate (BioRAD, Hercules CA, USA) before being visualised using a UVP BioSpectrum Imaging System (UVP, Upland, CA, USA).

Chapter 3: Results and Discussion

3.1 Investigation of the oligomeric state of the R3 fragment of RBBP6 and putative monomerising mutants

Retinoblastoma Binding Protein 6 (RBBP6) is a RING finger-containing E3 enzyme implicated in poly-ubiquitination of a number of cancer-associated proteins, including p53 (Li *et al*. 2007, Chen *et al*. 2013). A number of E3s have been shown to form homo-dimers through their RING finger domains, and it has been suggested that dimerisation is required for ubiquitination activity (Tanimura *et al*. 1999; Okamoto *et al*. 2005; LeBron *et al*. 2006; Cheng *et al*. 2011). The structure of the RING finger from RBBP6 has previously been solved using Nuclear Magnetic Resonance spectroscopy (NMR) and shown to homo-dimerize along the same interface found in many RING fingers (Kappo *et al*. 2012).

The dissociation constant, K_D, of the interaction was determined in the same study and found to be in the order of 100 µM.This means that at concentrations above 100 µM it is expected to be predominantly homo-dimeric whereas at concentrations below 100 µM it is expected to be primarily monomeric. The same study identified two single amino acid substitutions - N312D and K313E – located within the dimerisation interface that are able to abolish the homo-dimerisation of the RING finger (Kappo *et al*. 201).

A K_D of 100 µM corresponds to a weak interaction that is unlikely to be biologically relevant since the concentration of RBBP6 is unlikely to reach 100 µM. The possibility exists, however, that, as is the case with other E3s, parts of RBBP6 outside of the RING may contribute to the dimerisation interface, in which case the K_D of the complete molecule may be significantly less than 100 µM.

Full-length RBBP6 is too large and poorly structured to be suitable for expression in bacteria. The first aim of the project was therefore to express a larger fragment of RBBP6 containing the RING finger and use analytical size exclusion chromatography to investigate whether it formed monomers or homo-dimers. Co-workers in the laboratory had previously expressed an N-terminal fragment corresponding to the first 335 residues of RBBP6. It was dubbed R3 because it contained three recognisable domains: the ubiquitin-like DWNN domain, the zinc

finger, and the RING finger. R3 has been shown to be active as an E3 ubiquitin ligase (A. Faro, L. Jooste and D.J.R. Pugh, manuscript in preparation).

Two mutations that monomerize the RING finger, N312D and K313E, had previously been identified (Kappo *et al.* 2012). On the assumption that R3 would homo-dimerize more strongly than the isolated RING, the next step was to test whether the mutants were still able to monomerize R3. If not, it would demonstrate that R3 homo-dimerizes more strongly than the isolated RING and homo-dimerisation of R3 may therefore be biologically meaningful. The mutants would also represent useful negative controls for investigating the requirement for dimerisation on the ubiquitination activity of R3.

3.1.1 Insertion of putative monomerising mutations into the R3 fragment of RBBP6

The pGEX-R3-6His expression construct, containing cDNA coding for the first 335 residues of RBBP6 cloned into the *BamHI* and *XhoI* sites of pGEX-6P-2, had been generated previously by a co-worker, Dr Andrew Faro. The sequence was codon-optimised for expression in bacteria and included a 6His affinity tag inserted between R3 and the *XhoI* site, for affinity purification on nickel sepharose. In order to investigate whether the mutations N312D and K313E, along with an additional F313W mutant, were sufficient to abolish the expected homo-dimer adopted by the R3 fragment, the same mutations were introduced into the pGEX-R3-6His construct.

Table 3.1: Primers designed to generate mutated R3

Primer Name	Sequence
pGEX-6P-R3-N312D-F	5'-GAC GCA CTG ATT GCT GAC AAA TTT CTG CGC C-3'
pGEX-6P-R3-K313E-F	5'-GCA CTG ATT GCT AAC GAA TTT CTG CGC CAG G-3'
pGEX-6P-R3-F314W-F	5'-CTG ATT GCT AAC AAA TGG CTG CGC CAG GCT GTC-3'

The reverse primers are the reverse compliments of these forward primers.

Site-directed mutagenesis was carried out using the QuikChange protocol: briefly, the complete closed circular template was amplified using *Pfu*Turbo DNA polymerase (Agilent Technologies, Santa Clara, California), which is optimized for long and accurate reads. To minimize mutations, the protocol uses only a small number of cycles to amplify a small

number of copies and then selects for those few copies using a restriction enzyme, *DpnI*, that only cleaves its consensus sequence, 5´-GATC-3´, when it is methylated or hemi-methyated on the N6 position of the adenine (5´-Gm⁶ATC-3´). The template DNA is methylated, provided it was expressed in a *dam+ E. coli* strain, and so is cleaved by the enzyme, whereas the PCR amplicons are not methylated, and hence will not be cleaved and will transform into a cloning strain of *E. coli*.

Nine colonies were obtained for N312D, 12 for K313E and 13 for F314W. Plasmid DNA was extracted from six colonies for each mutant and four of each mutant were subjected to sequencing and found to contain the desired mutation, except two, one from K313E and one from F314W. Details of the sequencing can be found in the appendix section.

3.1.2 Bacterial expression and purification of wild type and mutant R3

Wild type R3 (residues 1-335 of human RBBP6) containing an N-terminal GST and a C-terminal 6His tag was expressed at 30 °C in *E. coli* BL21(DE3)pLysS using the pGEX-6P-2 expression vector. As can be seen from Figure 3.1, panel A, a protein of greater than 70 kDa was eluted from the column after addition of reduced glutathione (lanes 7-11), accompanied by a number of lower molecular weight species. This is larger than the expected size of 64.7 kDa, as determined using the ProtParam server (http://web.expasy.org/protparam/); the reason for this is not known, but may have to do with the fact that the protein forms a homo-dimer (see below). The isolated RING finger has been reported to migrate at almost twice its expected molecular weight (Kappo *et al*. 2012).

In an attempt to remove the lower MW bands, the fusion protein was subjected to HisTrap chromatography using the C-terminal 6His tag. Due to the position of the tag, only proteins with an intact C-terminus will be retained and since the C-terminus is more likely to be subject to proteolysis than the N-terminus, which is made up of GST, this method may be expected to eliminate most of the lower molecular weight bands.

As can be seen from panels B and C of Figure 3.1, GST-R3-6His was retained on the nickel sepharose column and eluted in a sharp peak on the chromatogram (panel B, peak 3), corresponding to lanes 5-8 on the SDS-PAGE shown in panel C. This produced a significant

concentrating of the target protein, which was very convenient. However, there was no significant reduction in the fraction of lower molecular weight proteins. The reason for this is not clear; however since they co-elute with Full-length GST-R3-6His in both glutathione and nickel affinity chromatography, a likely explanation is that the lower MW bands correspond to fragments of R3, which dimerize with the full-length protein.

Fractions from Peak 1 in Figure 3.1 panel B were pooled together and GST was removed using 3C protease as shown in Figure 3.2, panel A. Cleavage was very efficient, producing a band at around 50 kDa, which is likely to correspond to R3-6His, and a stronger band around 28 kDa, which is likely to correspond to GST. The higher MW band is larger than expected for R3-6His (38 kDa, including the 6His tag and the five residues Gly-Pro-Leu-Gly-Ser left over after removal of GST using 3C protease), but is it consistent with the earlier observation that the fusion protein migrates at a higher molecular weight than expected. In fact, during the course of this work R3-6His was observed to migrate at a number of different effective molecular weights (data not shown). Size exclusion chromatography was used to remove GST after cleavage, as shown in panel B, yielding three well-separated peaks. SDS-PAGE analysis (panel C) shows that peak 2 consisted mainly of R3-6His and peak 3 of GST, resulting in effective separation of proteins. Fractions making up peak 2 were pooled and used to investigate the oligomerisation state of wild type R3 (see below). Using the expression constructs generated earlier, the N312D, K313E and F314W mutants were expressed in the same way and successfully purified (data not shown).

3.1.3 Expression and purification of the RING finger from RBBP6

Samples of the isolated RING (249-335 of human RBBP6), wild type, and N312D and K313E mutants were also expressed using existing expression constructs, to serve as positive controls for the analytical SEC analysis of R3. Previous analysis using NMR showed conclusively that the N312D and K313E mutants of the isolated RING are monomeric, whereas the wild type is only partially dimeric at NMR concentrations (between 0.2 and 1 mM).
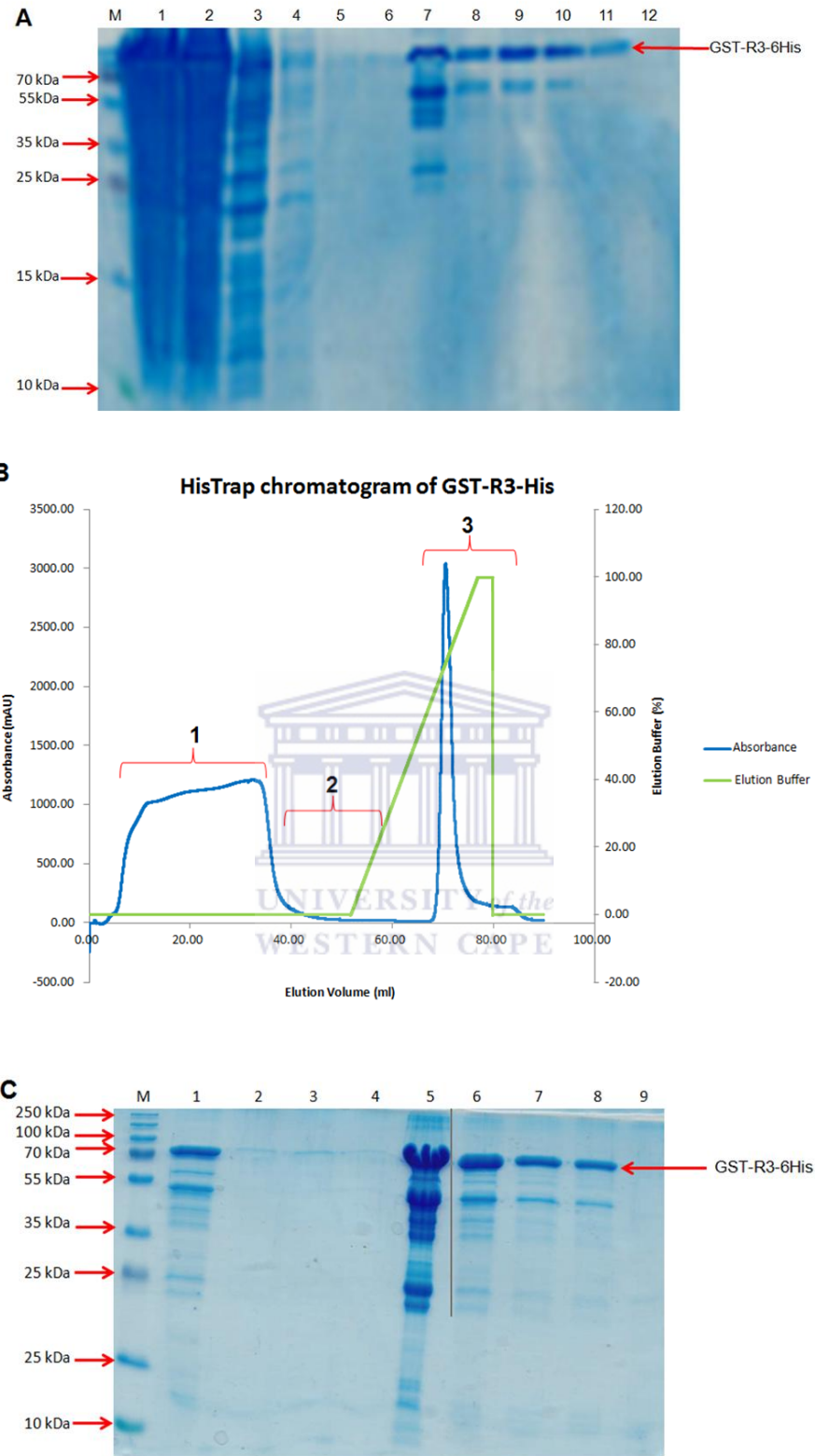
Figure 3.1: Purification of the fusion GST-R3-6His. (A) Purification using a gravity-flow glutathione agarose column. Lane M shows the protein molecular weight marker, lane 1 the insoluble protein, and lane 2 the soluble (crude) lysate. Lane 3 is the flow through, lanes 4-6 are washes and lane 7-11 shows fraction eluted from the glutathione-agarose column. Lane 12 shows fraction during NaCl wash. (B) Purification using HisTrap chromatography. Peak 1 is the flow through and peak 3 is the elute fractions. (C) The SDS-PAGE substantiates the HisTrap chromatogram, lanes 2-4 show the flow through (peak 1) and lanes 5-9 shows elution fraction (peak 3).
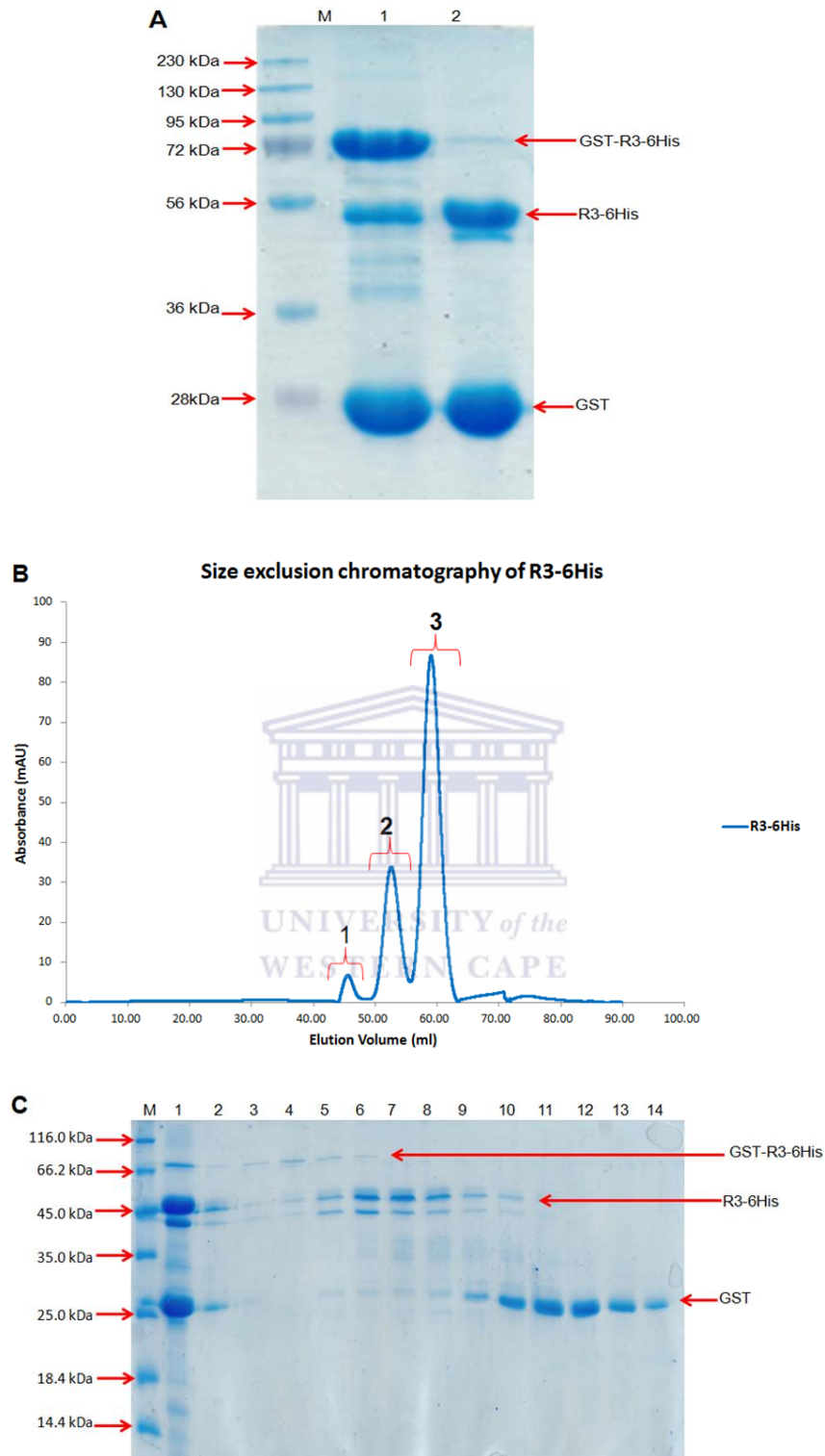
Figure 3.2: Purification of R3-6His after removal of GST. (A) Some in-cell cleavage of the fusion protein around the 72 kDa were observed in Lane 1; nevertheless the GST was completely removed after cleavage with 3C protease (lane 2) yielding bands around 50 kDa and the 25 kDa corresponding to R3 and GST respectively. (B) Size exclusion chromatogram showing clear separation between R3-6His (peak 2) and GST (peak 3) (C) The Coomassie stained SDS-PAGE of the SEC samples from the three peaks, lanes 2-4, lanes 5-8 and lanes 9-14 represented peak 1, 2 and 3, respectively.

Panel A of Figure 3.3 shows that large amounts of pure GST-RING were successfully eluted from the glutathione agarose column (lanes 6-8). The absence of a prominent band in the insoluble fraction (lane 2) confirms that the isolated RING is highly soluble, as reported previously (Kappo *et al.* 2012). After the cleavage of the fusion protein with 3C protease, lane 2 of panel B, which is produced recombinantly in our laboratory, yielded the expected band at around 15 kDa corresponding to RBBP6-RING, as well as a band corresponding to GST at around 27 kDa. It has been observed previously that the RBBP6-RING finger typically migrates as a smear between 10 and 20 kDa (Kappo *et al.* 2012). The significant band at around 37 kDa corresponds to un-cleaved fusion protein, showing that cleavage with 3C was not 100 % successful. The band around 50 kDa in lane 2 of panel B corresponds to the GST-3C fusion protein.

Following dialysis to remove free glutathione the cleaved sample was returned to the glutathione-agarose column to remove free GST, fusion protein and GST-3C protease (lanes 7-8), with RBBP6-RING being collected in the flow through (lanes 3-4). This was only partially successful, with a significant fraction of GST and fusion protein remaining in lanes 3 and 4 (see panel C of Figure 3.3).
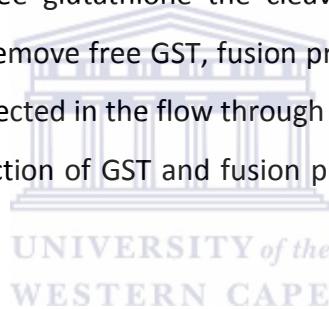
Remaining GST and GST-RBBP6-RING were successfully removed using size exclusion chromatography. Two well-separated peaks were obtained, as shown in the chromatogram in panel C, with peak 1 corresponding to GST and peak 2 to RBBP6-RING. Panel C shows that the end result was a strong, highly purified sample of RBBP6-RING. Samples of the N312D and K313E mutants of RBBP6-RING were prepared similarly from pre-existing expression constructs (data not shown).

3.2 Investigation of the oligomeric states of the RING finger and R3 fragments of RBBP6

Size exclusion chromatography separates molecules based on their effective molecular weight. A linear relationship is observed between the elution volume (Ve) and the logarithm of the molecular weight, $\log_{10}$(MW), over a range of MW that depends on the beads making up the matrix. This relationship can be used to give reasonably good estimates of the effective molecular weight of protein by comparing it with a standard curve generated using
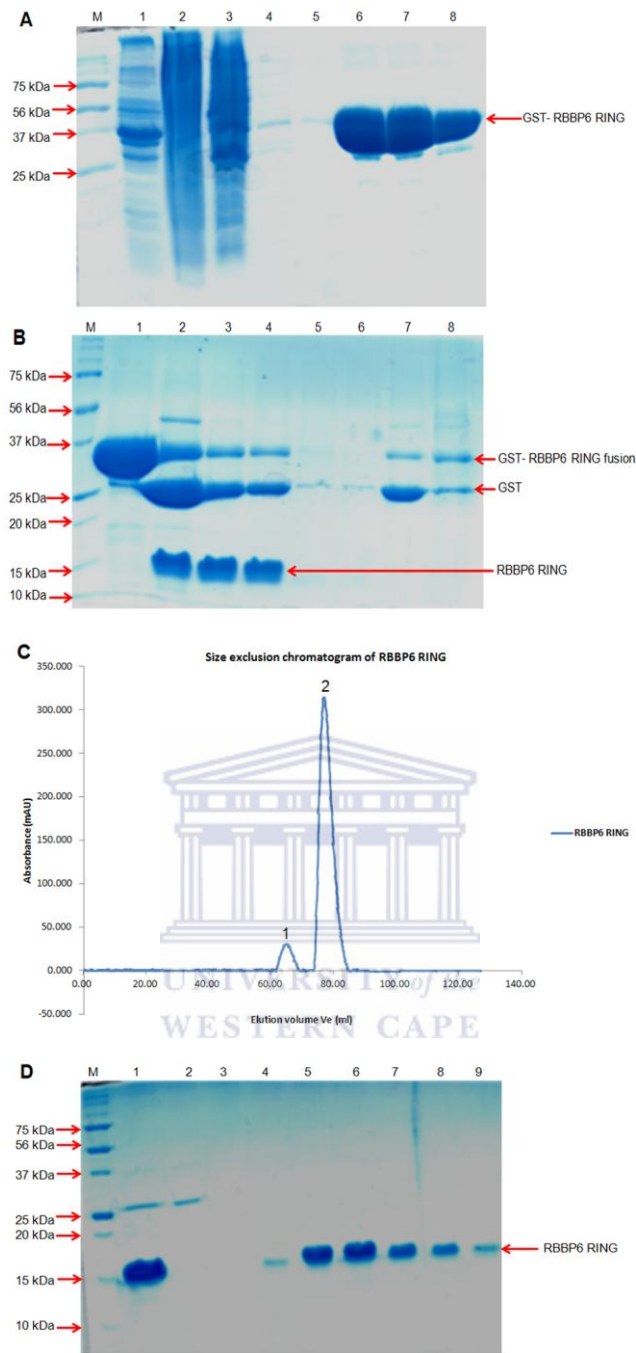
Figure 3.3: Expression and purification of the RING finger from RBBP6. (A) Cell lysate of the GST fusion RING finger was purified using glutathione-agarose column. The large amount of the fusion protein at around 37 kDa was expressed; lanes 6-8 show the eluted fraction. Lane 1 shows the soluble fraction and lane 2 is the insoluble fraction. Lane 3 is the flow through and lanes 4-5 show the washes. (B) Following cleavage of the GST tag, GST was removed using a glutathione-agarose column, with the target protein being collected in the flow through. Lane 2 is the sample after cleaving, showing bands at around 37 kDa and 15 kDa corresponding to the GST-RING finger and the RING finger, and bands around 50 kDa and 25 kDa corresponding to the GST-3C protease and free GST, respectively. Lanes 7 and 8 shows the GST tag and fusion protein eluted from the column. This step was repeated three times to separate GST and the fusion protein from the protein of interest. (C) Size exclusion chromatogram showing clear separation between GST (peak 1) and RBBP6-RING (peak 2) (D) SDS-PAGE confirming the peaks. Lanes 2-3 shows fractions from peak 1 and lanes 4-9 shows fractions from peak 2.
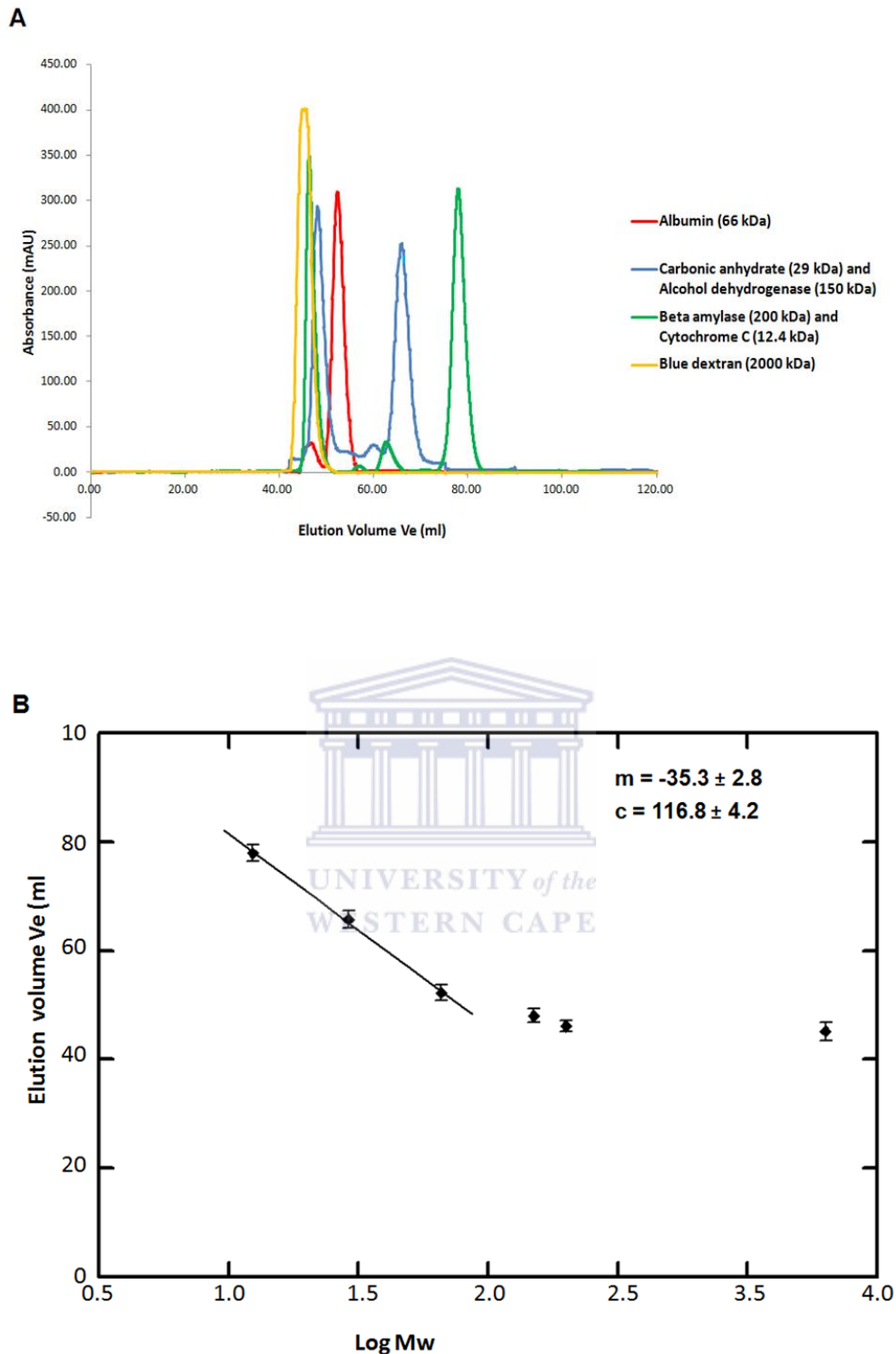
Figure 3.4: Protein standards used to estimate molecular weight. (A) Size exclusion chromatogram of protein standards shown in different colours. Proteins with molecular weight (MW) above the MW range between 3 kDa and 70 kDa of the matrix eluted in or just before the void volume, around 45 ml. These proteins include Alcohol dehydrogenase (150 kDa) and Beta-amylase (β-amylase) (200 kDa). (B) Standard curve of elution volume (Ve) against the log (MW) for protein standards. Cytochrome C (12.4 kDa), Carbonic Anhydrase (29 kDa) and Albumin (66 kDa), were used to form a straight line. While the point that level off, Alcohol dehydrogenase (150 kDa) and Beta (β)-amylase (200 kDa) were excluded, including the Blue dextran (2000 kDa).

proteins of known molecular weight. This is an effective method of determining whether proteins are monomeric, dimeric, or oligomeric in solution.

3.2.1 Calibration of the SEC column

The proteins listed in Table 3.2 were used to generate a standard curve for a HiLoad 16/60 Superdex 75 column. The elution volumes are recorded and the chromatogram is shown in Figure 3.4, panel A. A graph of Ve *vs* log (MW) is shown in panel B. The data lie on a straight line for the three proteins up to 66 kDa, but for higher molecular weight proteins, the graph flattens out. This is as expected, since Superdex 75 is only expected to be linear up to approximately 75 kDa. Only the first three points were therefore fitted to a straight line, yielding slope m = 35.3 ± 2.8 and y-intercept c = 116.8 ± 4.2.

Table 3.2: Molecular weights and elution volumes for proteins used to construct a standard curve

Protein Standards	Molecular Weight (kDa)	Log (Mw)	Elution Volume (ml)
Cytochrome C	12.4	1.09	77.9
Carbonic anhydrase	29	1.46	65.7
Albumin	66	1.82	52.3
Alcohol dehydrogenase	150	2.18	48.0
β-Amylase	200	2.30	46.2
Blue dextran	2000	3.30	45.2

3.2.2 SEC analysis of wild type and mutant RBBP6-RING

RBBP6-RING was previously shown using NMR spectroscopy to form a homo-dimer with a K_D of around 100 μM (Kappo *et al*. 2012). This means that at concentrations much above 100 μM it is expected to be dimeric whereas at concentrations much below 100 μM it is expected to be monomeric. The same study showed that two single amino acid substitutions within the dimerisation interface - N312D and K313E - were able to monomerize RBBP6-RING. Figure 3.5 shows that RBBP6-RING wild type, N312D and K313E eluted around 76.35 ml, 82.54 ml, and 82.74 ml respectively. Employing the parameters extracted from the standard curve this corresponds to an effective molecular weight of 13.98 kDa for wild type RING, and 9.34 kDa and 9.23 kDa for N312D and K313E respectively (see Table 3.3).

The values for the mutants agree well with the expected molecular weights of 9.2 kDa, confirming that they are indeed monomers. The value obtained for the effective MW of the wild type falls approximately half way between the weights of the monomer and homo-dimer. This is not a surprise because the loading concentration of approximately 81 μM is of the same order as the K_D (100 μM) and consequently each molecule is likely to spend part of its time on the SEC column as a monomer and part as a dimer. As a result, it is likely to elute somewhere between the volumes expected for a monomer and a dimer, which is exactly what is observed. These results are therefore consistent with the results of the previous NMR study. These results suggest that size exclusion chromatography can be used to determine the molecular weight of proteins. However, it is more useful and reliable if coupled with multi angle light scattering (SEC-MALS), which overcomes the limitations of column calibration and determine the molecular weight of protein directly (Meyer and Morgenstern 2003, Lauber *et al*. 2015).
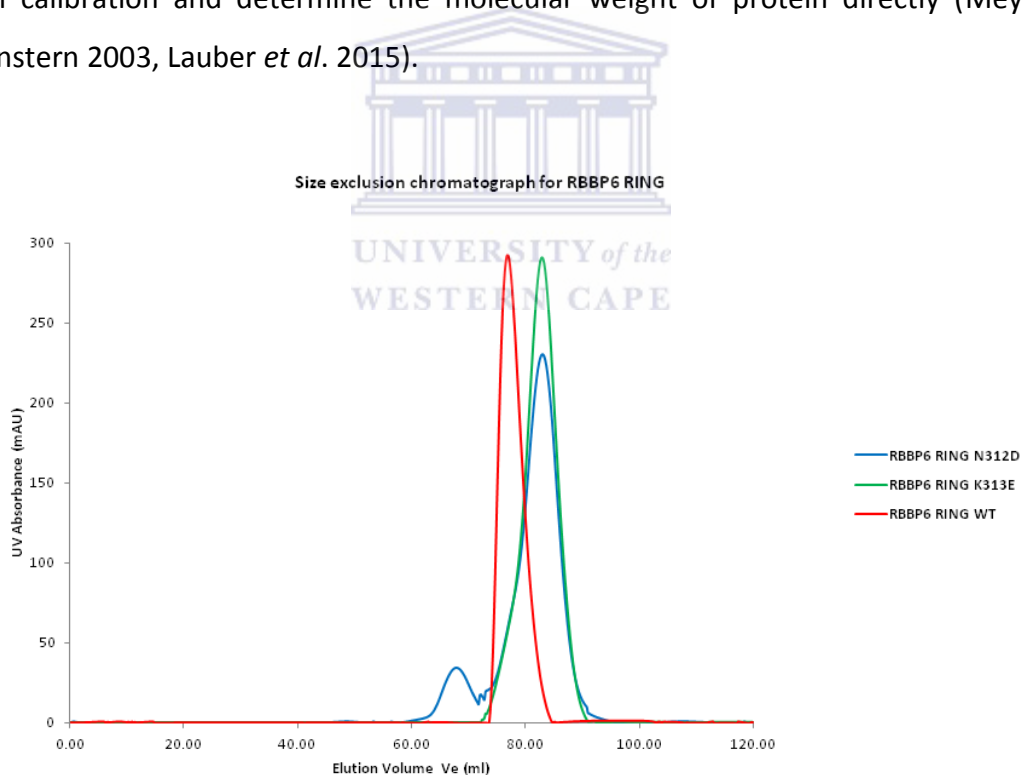
Figure 3.5: Size exclusion chromatogram of the wild type and mutated RING finger from RBBP6. Both mutants RING-N312D and K313E eluted at around 80 ml, corresponding to a molecular weight (MW) of approximately 9 kDa, showing that they are monomeric. In contrast, the wild type eluted at around 76 ml, corresponding to a MW of 14 kDa, which shows that it is partially monomeric and partially dimeric in solution, consistent with a previous NMR study.

Table 3.3: Determination of the effective molecular weight (MW) of RBBP6-RING

RBBP6 RING	Ve	Log MW	MW (kDa)
Wild type (WT)	76.4	1.15	14.0
N312D	82.5	0.97	9.3
K313E	82.7	0.96	9.2

3.2.3 SEC analysis of wild type and mutant R3

Next, we investigated the effective MW of wild type R3 and two mutant forms, N312D and K313E. In all cases, the loading concentration was approximately 84-87 µM. The chromatogram in Figure 3.6 shows that wild type R3 eluted at approximately 50 ml, which corresponds to 77.7 kDa using the calibration discussed earlier. This is consistent with the weight of the homo-dimer—38 kDa x 2 = 76 kDa—from which we conclude that R3 is entirely dimeric under these conditions (see Figure 3.6). Mutants, N312D and K313E eluted at essentially the same volume, from which we conclude that the same mutations that monomerize the RING are insufficient to monomerize the R3 dimer (see Table 3.5). We conclude from this that R3 is a stronger dimer than the isolated RING finger, and we therefore expect the K_D of the dimerisation to be smaller than the 100 µM measured for the RING finger. Whereas an interaction with a K_D of 100 µM is unlikely to be physiologically significant, since the concentration of RBBP6 is unlikely to reach 100 µM under physiological conditions, our results suggest it is possible that isoforms of RBBP6 larger than just the RING finger will dimerize sufficiently strongly to be physiologically relevant.

3.3 Expression and purification of the R2 fragment of RBBP6

The R3 fragment was found to be highly susceptible to proteolysis, as shown above, and so we sought to express a smaller fragment that may be more suitable for structural analysis. Alignment of RBBP6 orthologues from a number of organisms revealed the presence of a poorly conserved and low-complexity region between the DWNN domain and the zinc finger domain. This suggested the zinc and RING fingers, a fragment that we dubbed R2 because it contains only two domains, may form a structured unit. If so, we would like to investigate whether it formed a strong homo-dimer like R3, since that would suggest that R2 contains most of the dimerisation interface and that the DWNN domain is not required for dimerisation. In addition to the benefits for structural analysis, the proposed fragment may
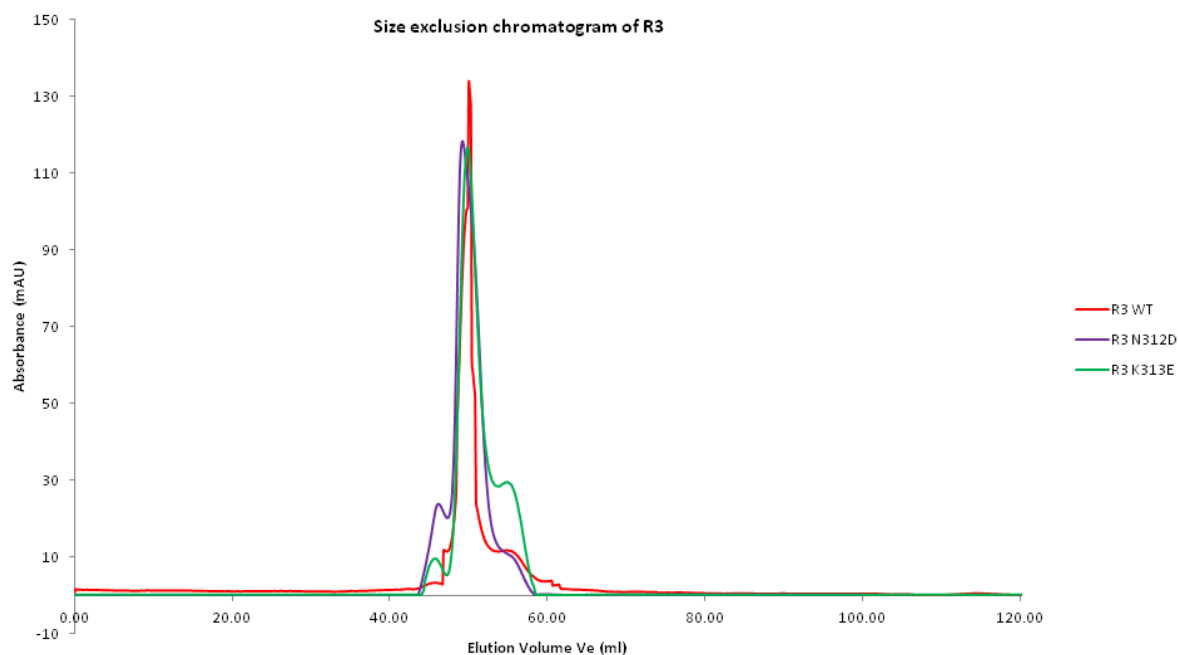
Figure 3.6: Size exclusion chromatogram of the wild type and mutated R3. The wild type and both mutants eluted around 50 ml, corresponding to a molecular weight of approximately 78 kDa. This is consistent with the weight of the homo-dimer, 74.8 kDa. The mutants were not sufficient to break homo-dimerization of the protein.

Table 3.4: Determination of the effective molecular weight (MW) of wild type R3 and two mutants

R3	Ve	Log MW	MW
Wild type (WT)	50.07	1.89	77.7
N312D	49.49	1.91	80.7
K313E	49.74	1.90	79.3

also be useful for investigating the requirement of dimerisation for ubiquitination and the role of the ubiquitin-like DWNN domain in ubiquitination. We had previously shown that R3 is active as an E3 ligase (A. Faro, L. Jooste and D.J.R. Pugh, manuscript in preparation); carrying out similar assays using R2 should show whether the DWNN domain was required for ubiquitination activity.

3.3.1 Generation of expression construct for R2-6His

The C-terminal end of the DWNN domain was at residue 81 and the start of the zinc finger in the vicinity of residue 160. Alignment of a number of RBBP6 orthologues showed that the region between residues 90 and 140 was poorly conserved and of low complexity, which

suggested that this might play the role of a flexible linker. The beginning of R2 was therefore chosen at residue 143. Oligonucleotide primers (see Table 3.5) were designed to amplify residues 143 – 335 of RBBP6, using a codon-optimised cDNA coding for the R3-6His previously synthesised by GenScript Inc. (Piscataway NJ, USA) and supplied in a pUC57 vector. Since the pET28a vector includes a C-terminal 6His tag that cannot be conveniently removed, the primers were designed to exclude the 6His tag in the template, and to incorporate an *XhoI* site in order to utilise the 6His tag in the vector. The forward primer was designed to incorporate an *NcoI* site to eliminate the N-terminal 6His tag present in the vector. The beginning of R2 (Asp-Pro-Ile-Asn-) followed immediately after the first four residues (Met-Gly-Ser-Ser) expressed from the pET28a promoter. At the C-terminus of R2 (-Leu-Arg-Lys-Gln) an additional pair of residues (Gly-Ser) was inserted (in addition to the -Leu-Glu- already present) immediately before the 6His tag in order to ensure that the 6His tag was not too close to R2 to interfere with its ability to bind to nickel sepharose. The construct was designed to express a 207 amino acid protein with an expected molecular weight of 23.0 kDa (ProtParam server http://web.expasy.org/protparam/) (Gasteiger *et al*. 2005).
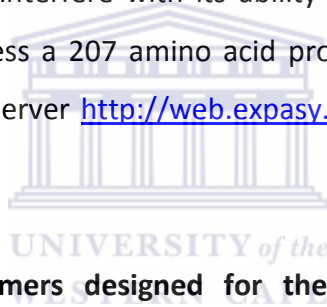
Table 3.5: Oligonucleotide primers designed for the generation of pET28a-R2-6His construct

Primer Name	Sequence
pET28a-R2-F	5'- GAG GCG CCA TGG GCA GCA GCG ACC CGA TCA ACT ACA TGA AA -3'
pET28a-R2-R	5'- GAG GCG CTC GAG GCT GCC TTG TTT ACG CAG ACG TTT CGT -3'

Bases highlighted in pink and green correspond to *NcoI* and *XhoI* restriction sites respectively; blue code for the "spacer-residues" Gly-Ser inserted between the C-terminus of R2 and the 6His tag. Underlined bases are complimentary to the insert. No stop codon is included so that the 6His tag contained in the plasmid will be incorporated into the expressed protein.

Successful generation of the pET28a-R2-6His construct is shown in Figure 3.7. The R2 insert was successfully amplified by PCR, yielding a band consistent with the expected size of approximately 600 bp (panel A, lane 2). The expression vector and the amplicon were digested with *NcoI* and *XhoI* to generate complementary sticky ends (panels B and C respectively) after which they were ligated and transformed into *E. coli*. Plasmid DNA from putative transformants was digested with *NcoI* and *XhoI* to release the insert, as shown in panel D. Released fragments of the expected size can be seen in lanes 3, 5, 7, 9 and 11; the
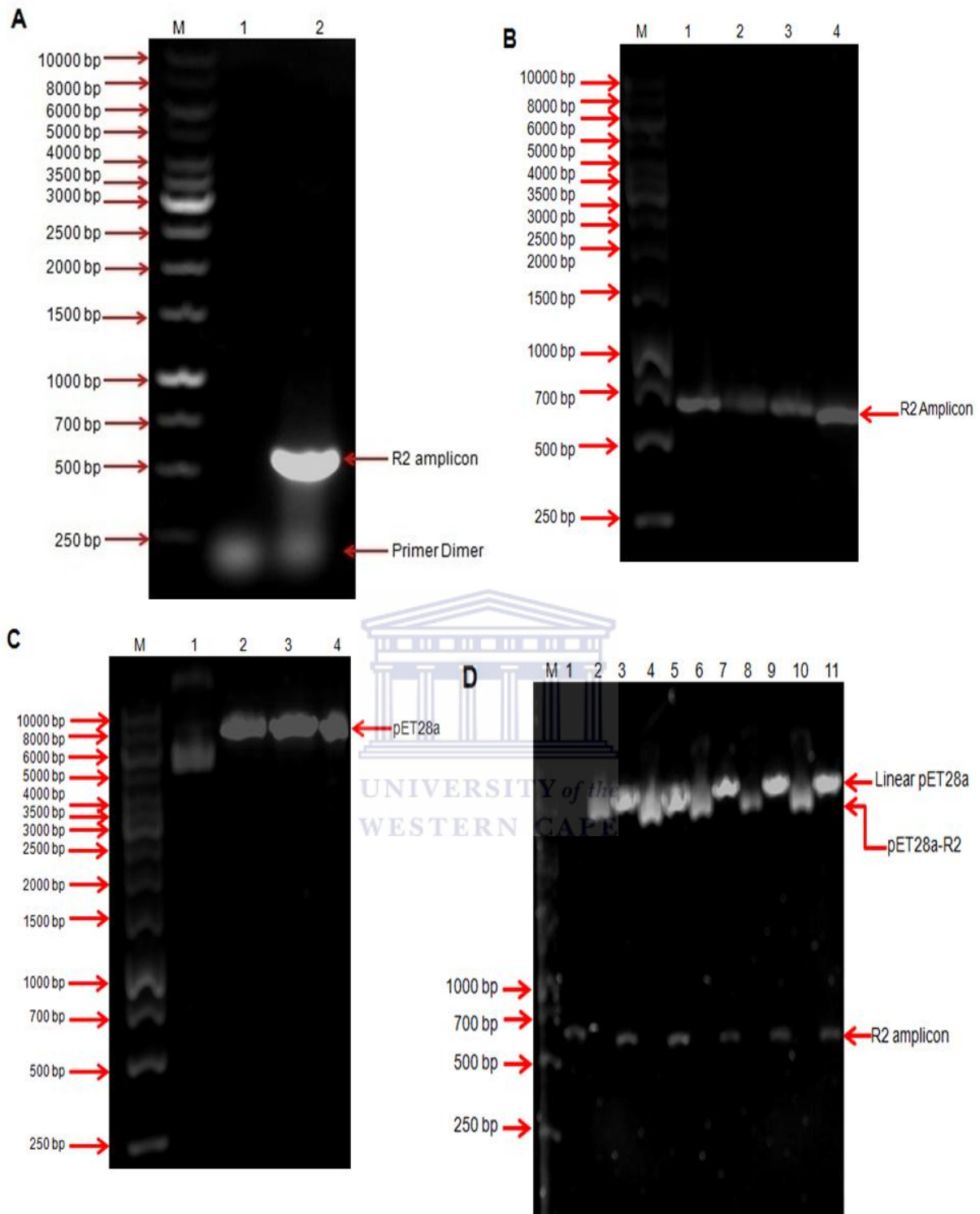
Figure 3.7: Generation of pET28a-R2-6His expression constructs. (A) The band at approximately 600 bp in lane 2 corresponds to the desired R2-6His amplicon and lane 1 is the negative control. (B) Digestion of R2 amplicon using both NcoI (lane 2) and XhoI (lane 3), whereby lane 4 is the double digested R2 amplicon with the same enzymes, whilst Lane 1 is the undigested R2 amplicon (C) Digestion of pET28a expression vector using both NcoI (lane 2) and XhoI (Lane 3) and lane 4 is the double digest. Lane 1 is the circular vector. (D) Screening of putative positive colonies: lane 3, 5, 6, 7, and 9 are double digests of the recombinant DNA. Lane 1 consists of an R2 amplicon as a control and lane 2, 4, 6, 8 and 10 are controls.

original PCR amplicon loaded in lane 1 indicates the approximate size of the insert. The DNA sequence of the colonies was confirmed by direct DNA sequencing.

3.3.2 SEC analysis of R2

SEC was used to determine the effective MW of R2 (143-335 of human RBBP6) using a loading concentration of approximately 90 µM. Figure 3.11 shows that R2 eluted at around 58 ml, which corresponds to a MW of 46 kDa (see Table 3.6). A molecular weight of 46 kDa agrees very well with the expected MW of homo-dimeric R2: 2x 23 kDa = 46 kDa. We conclude that, like R3, R2 forms a strong homo-dimer. This result supports the conclusion that the zinc knuckle participates in the homo-dimerisation interface, increasing the affinity of the interaction when compared to the isolated RING. It further suggests that the DWNN domain may not play a role in the homo-dimerisation, a possibility that warrants further investigation.

3.4. *In vitro* investigation of auto-ubiquitination of the RING finger domain from RBBP6

Many ubiquitin E3-ligases are able to catalyse ubiquitination of themselves as well as substrates, a process known as auto-ubiquitination (Everett *et al.* 2010). Auto-ubiquitination is often used as a convenient proxy for substrate-ubiquitination, both because it is easier to study *in vitro* and because substrates for a particular E3 are not always known.

RBBP6 has been shown to be able to ubiquitinate substrates such as YB-1 (Chibi *et al.* 2008), zBTB38 (Miotto *et al*. 2014) and p53 (Dr A. Faro, Ms L. Jooste and Dr D.J.R. Pugh, unpublished data) but prior to this work the question of whether RBBP6 could auto-ubiquitinate itself had not been investigated fully. Preliminary un-published results obtained by a co-worker suggested that the isolated RING finger domain was able to auto-ubiquitinate itself *in vitro*, leading to degradation in the proteasome (Dr A. Faro and Dr D.J.R. Pugh, manuscript in preparation); auto-ubiquitination of RING fingers has been previously reported by Everett and co-workers (Everett *et al.* 2010). We therefore decided to attempt to replicate the result using wild type RBBP6-RING as well as the monomerising mutants. Homo-dimerization is known to be a requirement for ubiquitination activity of many E3s, so it would be of interest to determine whether the mutants catalysed auto-ubiquitination as efficiently as wild type.
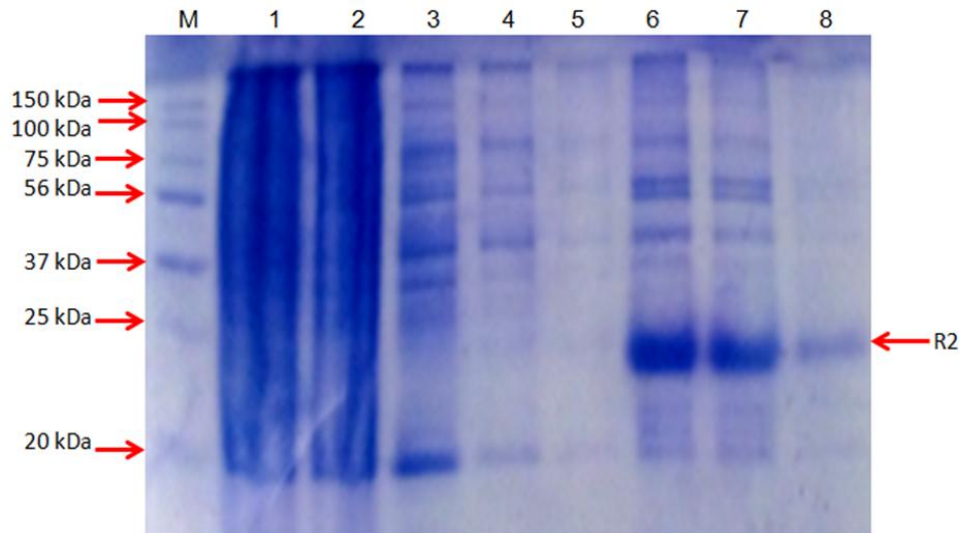
Figure 3.8: Expression and purification of R2 using a nickel sepharose column. Protein retained by the column and subsequently eluted can be seen in lanes 6-8.
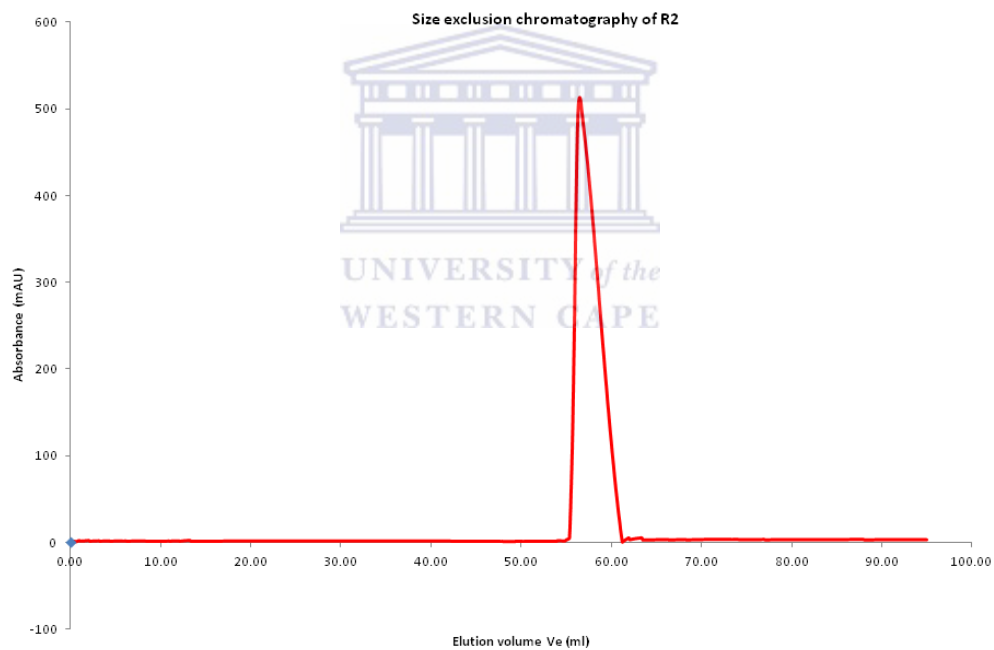
Figure 3.9: Size exclusion chromatography of R2. R2 protein eluted at around 58 ml, which corresponds to a molecular weight of 46 kDa. The molecular weight of 46 kDa agreed very well with the expected homo-dimeric MW of 46.0 kDa (2x 23.0 kDa).

Table 3.6: Determination of the effective molecular weight (MW) of R2

R2	Ve	Log MW	MW
Wild type	58.01	1.67	46.3

Bacterially expressed wild type RBBP6-RING was subjected to *in vitro* ubiquitination assays

using the following enzymes kindly supplied by co-workers in the laboratory, Ms L. Jooste

and Dr A. Faro: human E1, the E2s UbcH1, UbcH5a, UbcH5b, UbcH5c, UbcH6, UbcH7 and UbcH13 and HA-tagged ubiquitin. The protocol set out in Section 2.11, which makes use of the high stability of ubiquitin at low pH to precipitate other proteins, was required since HA-ubiquitin contained neither GST- nor 6His-tag for affinity purification. Ubiquitinated RBBP6-RING was detected by Western Blotting with antibodies targeting ubiquitin, rather than the more common strategy of targeting the HA tag with anti-HA antibodies.

Panel A of Figure 3.10 shows that wild type RBBP6-RING is able to auto-ubiquitinate itself in the presence of E1, E2 and ubiquitin (lane 6), but not when ubiquitin is omitted (lane 5), all E2s are omitted (lane 4) or E1 is omitted (lane 3). The ladder in lane 6 extends right up to the top of the gel, significantly past the top MW marker band at 150 kDa. Since RBBP6-RING contains only five lysine residues, mono-ubiquitination at each site would account for only 50 kDa, suggesting that the ladder corresponds to the formation of poly-ubiquitin chains. It is perhaps of concern that free ubiquitin is not also observed, migrating at 10 kDa, in all lanes to which it was added; i.e. lanes 2-4 of panels A, B and C. This is most likely to be the result of under-exposure of the image due to the heavy signal in lane 6; however, it warrants further investigation.
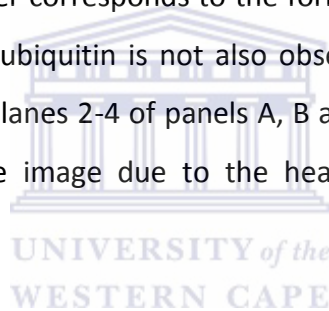
Panels B and C show that the N312D and K313E mutants are also able to auto-ubiquitinate themselves, ruling out the hypothesis that homo-dimerisation is required for ubiquitination. However the ubiquitination appears not to extend as far up the gel as with the wild type, which may be evidence that monomeric RBBP6-RING auto-ubiquitinates itself less efficiently or that it comprises mono-ubiquitination rather than poly-ubiquitination. Although RBBP6-RING was not demonstrated to self-ubiquitinate as an E3 ligase in previously studies. Immediate-early protein ICP0 of herpes simplex virus type 1 (HSV-1)-RING has been shown to self-ubiquitinate (Everett et al. 2010).

One of the most well known characteristics of poly-ubiquitination is its ability to catalyse degradation of the substrate protein in the 26S proteasome. This is most closely associated with lysine 48-linked chains, although other modes of linkage have also been reported to catalyse degradation (Zhang *et al.* 2013). In order to test whether the auto-ubiquitination of the RING finger rendered it susceptible to degradation, intact proteasomes precipitated

from mammalian cell lysates (a kind gift from a co-worker in the laboratory, Ms Tephney Hutchinson) were added to the reactions. Panel D of Figure 3.10 shows that addition of proteasome caused the high molecular weight ladder to disappear dramatically (compare lanes 1 and 2), suggesting that the RING has been degraded by the proteasome. The effect is less dramatic in the case of the mutants (compare lanes 3 and 4 and lanes 5 and 6 respectively), but it is still present.

A possible alternative explanation for the effect seen in panel D is that other factors such as de-ubiquitinating proteases (DUBs) have been inadvertently added to the reaction along with 26S proteasome. To control for this effect, an improvement of this assay would involve the addition of MG132 along with the proteasomal preparation. Since MG132 specifically inhibits the proteasome and not other proteases, if it were able to rescue the high molecular weight ladders it would constitute conclusive evidence that the disappearance of the bands was indeed due to degradation of RBBP6-RING by the proteasome.

3.5 *In-vitro* investigation of a putative interaction between the RING finger domains of RBBP6 and MDM2

RBBP6 has been reported to promote ubiquitination of p53 by MDM2 *in vivo*, leading to suppression of p53 (Li *et al.*, 2007). The authors of that report proposed that RBBP6 acts as a scaffold on which the complex of MDM2 and p53 assembles, involving the p53-binding domain identified towards the C-terminus of RBBP6 (Simons *et al*, 1997). However, preliminary results from our laboratory suggest that the R3 fragment of RBBP6 is sufficient to promote ubiquitination of p53 by MDM2. A possible alternative explanation is that RBBP6 forms a hetero-dimer with MDM2 through their respective RING finger domains, similar to the hetero-dimer formed between MDM2 and MDMX. To test this hypothesis we decided to express RBBP6-RING and MDM2-RING in bacteria and investigate whether they interacted *in vitro* using GST pull down assays. If so, this would lay the foundation for future NMR-based studies of the RING-RING complex.
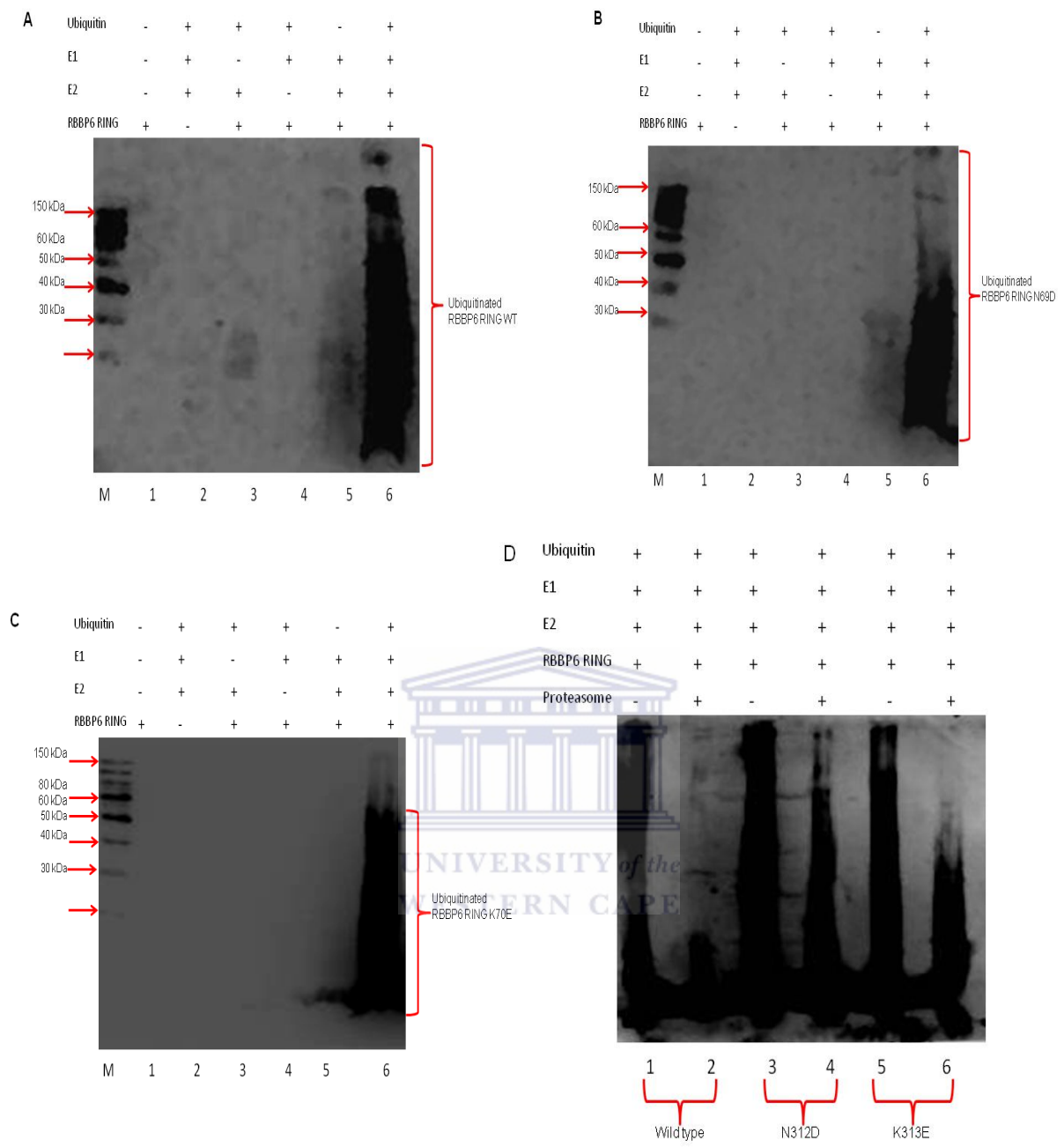
Figure 3.10: Auto-ubiquitination and proteasomal degradation of the isolated RING finger from RBBP6 *in vitro*. (A) Wild type RBBP6-RING is heavily ubiquitinated in the presence of ubiquitin, E1 and E2 enzymes (lane 6), but not when ubiquitin is omitted (lane 5), the E2 is omitted (lane 4) or the E1 is omitted (lane 3). Since no other E3 is present in this *in vitro* assay, it can only be auto-ubiquitination. Monomerising mutations N312D (B) and K131E (C) are similarly able to auto-ubiquitinate themselves, although possibly less efficiently than wild type. Polyclonal antibody sc-9133 from Santa Cruz Biotechnology Inc. (Santa Cruz CA, USA) raised against ubiquitin was used to detect the ubiquitinated RING. (**D**) Addition of intact proteasomes purified from human cell lysates dramatically reduced the higher molecular weight laddering, indicating that the auto-ubiquitinated RING had been degraded by the proteasome—compare lanes 1 (minus proteasome) and lane 2 (plus proteasome). A similar result was observed for the N312D mutant (lanes 3 and 4) and the K313E mutant (lanes 5 and 6), although the degradation did not appear to be as efficient as for wild type. A polyclonal antibody (sc-9133, Santa Cruz, CA, USA) raised against ubiquitin was used to detect ubiquitinated RING.

3.5.1 Expression and purification of the RING domains of RBBP6 and MDM2

RBBP6-RING was expressed as a GST-fusion protein and the GST tag was removed following purification, as described in Section 3.1.3. Constructs coding for the C-terminal RING finger domain of MDM2 (residues 438 to 491), fused to either a GST or a 6His tag (GST-MDM2-RING or MDM2-RING-6His respectively) had been previously generated by co-workers in the laboratory. Expression and purification of GST-MDM2-RING using a glutathione-affinity column is shown in Figure 3.11; significant quantities of pure protein were eluted from the column (panel A, lanes 6-8).

The fusion protein (panel A, lane 6-8, pooled together) (panel B, lane 1) was successfully cleaved using 3C protease, but relative to the amount of GST, the yield of MDM2-RING was significantly less than expected (panel B, lane 2). However, MDM2-RING has been reported to form oligomers including dimer and higher-order complexes *in viv*o (Cheng *et al*. 2011). Therefore, we suspect this resulted in high molecular weight ladders on SDS PAGE gels, which are difficult to observe, making the protein seem to disappear. Panel C shows purification of 6His-MDM2-RING using nickel ion affinity chromatography. Although it is not as clean as GST-MDM2-RING, a significant band around 15 kDa can be seen in lane 9.

3.5.2 Pull down assays involving the RING domains of RBBP6 and MDM2

GST-MDM2-RING was immobilized on glutathione-conjugated agarose beads and co-precipitation of RBBP6-RING was detected using a polyclonal antibody raised against bacterially expressed RBBP6-RING (produced in the laboratory of Prof Bellstedt, Biochemistry Department, Stellenbosch University). In colloquial terms, GST-MDM2-RING served as the "bait" and RBBP6-RING as the "prey". Note that although RBBP6-RING was originally expressed as a fusion with GST, GST was removed prior to the assay; otherwise, it would itself have been precipitated by the pull down procedure.

The band at the bottom of lane 4 corresponds to RBBP6-RING and shows that MDM2-RING is able to co-precipitate RBBP6-RING, whereas neither GST alone (lane 3), nor the glutathione-conjugated agarose alone (lane 2), were able to. The faint band at the bottom of lane 1 corresponds to the original diluted sample of RBBP6-RING, which had not been subjected pull down, which serves to confirm that the co-precipitated band in lane 4 is
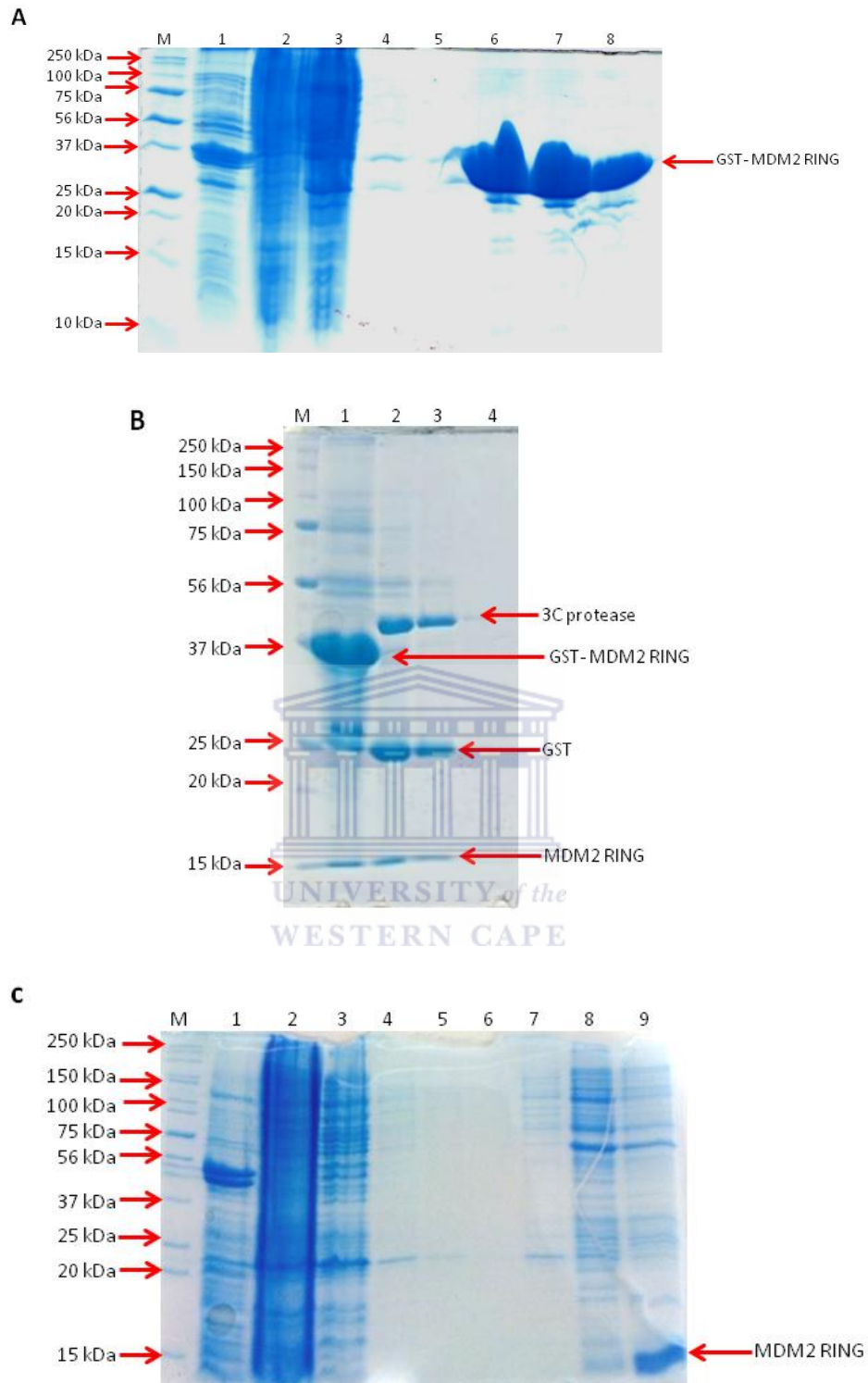
Figure 3.11: Expression and purification of MDM2 RING. (A) GST-MDM2 RING fusion retained in the glutathione-agarose column and eluted as indicated in lanes 6-8. The expression level of the protein in E.coli was quite good. Lane M: MW marker, lane 1: insoluble fraction, lane 2: soluble fraction, lane 3: flow through and lane 4-5: washes. (B) The fusion protein was successfully cleaved using 3C protease. M: MW marker, lane 1: before cleaving, lane 2: after cleaving, lane 3: flow through, lane 4: wash. (**C**) 6His-MDM2 RING-6 purified in Ni column, most protein eluted in lane 9. Lane M: MW marker, Lane 1: insoluble fraction, lane 2: soluble fraction, lane 3: flow through and lane 4-6: washes.

55

indeed RBBP6-RING. The higher molecular weight bands detected by anti-RBBP6-RING antibody in lane 4 of Figure 3.12 may be contaminant of un-cleaved fusion protein, as well as smears indicating oligomerisation of the RING.

The pull-down assay is an *in vitro* method used to determine a physical interaction between MDM2-RING and RBBP6-RING. Techniques such as yeast two-hybrid, GST pull-down, and co-immunoprecipitation, are usually used together to determine or verify the interactions of protein (Agarwal *et al*. 2008). Thus, this pull-down assay serves as an initial screening assay for identifying interaction between MDM2-RING and RBBP6-RING using co-immunoprecipitation and yeast two-hybrid.
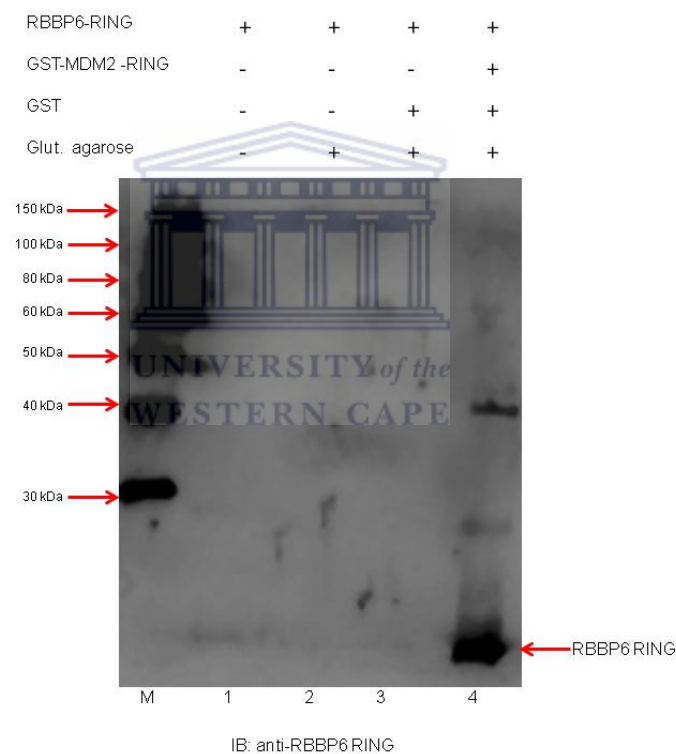
Figure 3.12: GST-MDM2-RING is able to precipitate RBBP6-RING. RBBP6-RING was co-precipitated by GST-MDM2-RING (lane 4), but not by GST alone (lane 3). It was also not precipitated by the glutathione-agarose alone (lane2). RBBP6-RING was detected using a RBBP6 polyclonal antibody (produced in the laboratory of Prof Bellstedt, Biochemistry Department, Stellenbosch University) raised against bacterially-expressed RING domain.

Chapter 4: Conclusions and outlook

4.1 Generation of shortenings of RBBP6 and investigation of their oligomeric states

In vitro analysis of the structure and ubiquitination activity of Retinoblastoma Binding Protein 6 (RBBP6) is dependent on efficient over-expression of RBBP6 in bacteria. Given the large size, the apparent modular nature of the protein and predictions that large parts of the protein are intrinsically unstructured, identification of fragments of RBBP6 that are large enough to contain the interesting activities such as ubiquitination, while at the same time small enough to be efficiently expressed, is essential. Prior to this work, a fragment denoted "R3" spanning the first 335 residues of RBBP6, and containing the DWNN, zinc finger and RING finger, had been successfully expressed in bacteria and shown to have E3 ubiquitination ligase activity. Many E3 ubiquitin-ligases have been found to form homo-dimers, and dimerisation is suspected to play a role in their catalytic activity. Previous results using protein Nuclear Magnetic Resonance Spectroscopy (NMR) showed that the RING finger domain of RBBP6 forms weak homo-dimers in solution, but that this could be effectively disrupted by single amino acid substitutions N312D and K313E (Kappo *et al*. 2012). The first aim of this work was to use analytical size exclusion chromatography (SEC) to investigate the oligomeric state of R3 and the corresponding mutants.

Before testing R3, a benchmarking study was carried out on the isolated RING finger and the above mutants. As expected both mutants were found to be monomeric, with apparent molecular weights very close to values (9 kDa) expected based on the primary sequence. The apparent MW of wild type RING, however, was found to be larger (14 kDa), consistent with the NMR-derived result that the RING is a mixture of homo-dimer and monomer at these concentrations.

In contrast, SEC showed that wild type R3 forms a strong homo-dimer, with most of the molecules forming part of homo-dimers, but that the N312D and K313E mutations are not sufficient to disrupt the homo-dimer. We conclude from this that the interface formed by R3 is larger than that formed by the isolated RING finger, and must therefore include parts of R3 outside the RING finger domain. It also suggests that the K_D of the dimerisation is smaller

than the 100 µM measured for the RING finger domain. This increases the likelihood that RBBP6 is dimeric under physiological conditions.

The above result posed the question: Which part of R3, in addition to the RING, formed part of the interface: the DWNN domain or the zinc finger? To address this question we attempted to design a further shortening of R3 excluding the DWNN domain. Based on inspection of an alignment of RBBP6 orthologues a start site of residue 143 was selected, between the end of the DWNN domain (residue 81) and the beginning of the zinc finger domain (residue 160). This fragment, denoted R2 because it contained 2 of the three domains identified in R3, was cloned into a pET28a vector so that it would be expressed with a C-terminal 6His affinity tag. The protein was successfully over-expressed in *E. coli* and shown, like R3, to form a strong homo-dimer. This suggests that the DWNN domain does not form part of the interface, nor is it required for correct folding of R2. Combined with results obtained by co-workers that R2 is able to catalyse ubiquitination as efficiently as R3, this suggests that R2 may be a more convenient system for structural investigation of the ubiquitination activity of RBBP6 than R3.

This study has laid the groundwork for future NMR-based investigation of the R2 fragment and the homo-dimer interface. Expression and purification of R2 should be optimised to produce as much protein as possible while minimising degradation as much as possible. ^{15}N- and ^{13}C-enriched samples should be expressed by growing the bacteria on minimal media supplemented with ^{15}N-ammonium chloride and ^{13}C-glucose as the sole nitrogen and carbon sources respectively. Assignment of backbone residues will be carried out using standard triple resonance experiments and residues forming part of a rigid structure (as opposed to flexible regions) will be determined using a ^{15}N-NOE spectrum. If necessary, flexible regions will be removed from the ends of the fragment and expression of the final construct will be optimised for NMR-based investigation of the structure of the homo-dimer.

4.2 Auto-ubiquitination of the isolated RING finger of RBBP6

Additional investigations were carried out using fragments of RBBP6 expressed for the above study. Auto-ubiquitination of E3s by themselves is a useful proxy for substrate ubiquitination, especially when it comes to identifying associated E2 enzymes and whether

the ubiquitination is poly- or mono-ubiquitination, and the mode of linkage of poly-ubiquitin chains. Prior to this project there was no published report of auto-ubiquitination of RBBP6 although our own preliminary data suggested that it does happen, leading to degradation in the proteasome. To our surprise, we found significant auto-ubiquitination of both wild type and monomeric RBBP6-RING in *in vitro* studies. Auto-ubiquitination of an isolated RING finger *in vitro* has been reported previously (Everett *et al*. 2010), but to our knowledge that is the only previous report. Auto-ubiquitination was observed not only with wild type, but also with the monomeric mutants N312D and K313E, although it is possible that auto-ubiquitination with the mutants is less efficient than with wild type. We deduce that auto-ubiquitination of the RBBP6 RING finger does not require homo-dimerisation, although it is possible that it is more efficient when the RING is dimeric. Importantly, the higher molecular weight species were significantly reduced when purified human proteasome was added, from which we conclude that the ladders represent poly-ubiquitination rather than multiple mono-ubiquitination, and that the chains are lysine48-linked. To our knowledge this is the first time that ubiquitin-catalysed degradation of a RING finger has been demonstrated *in vitro*.
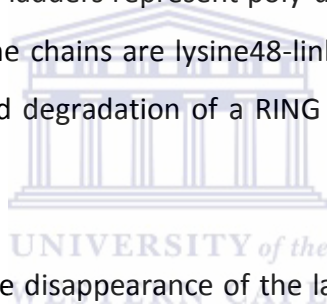
An alternative explanation for the disappearance of the ladders is that they were removed by de-ubiquitinating enzymes (DUBs) co-precipitated with the proteasome. In order to eliminate this possibility the assay needs to be repeated adding controls in which the proteasome inhibitor MG132 is pre-incubated with the lysate before addition of RBBP6-RING; if MG132 rescues the auto-ubiquitination then we can conclude that auto-ubiquitination of RBBP6-RING targets it for degradation in the proteasome.

4.3 Investigation of a possible interaction between the RING fingers of RBBP6 and MDM2

The final part of the thesis describes investigation of the interaction between the RING fingers of RBBP6 and MDM2 *in vitro*. The investigation was prompted by unpublished data from co-workers in our laboratory showing that the R3 fragment of RBBP6 is sufficient to activate MDM2 to catalyse poly-ubiquitination of p53; this raises the question of whether MDM2 hetero-dimerizes with RBBP6 through their respective RING finger domains in the same way that it hetero-dimerizes with MDMX. To test this model, the RING fingers from RBBP6 and MDM2 were expressed in bacteria and used in a GST pull down assay; GST-

MDM2-RING (the bait) was precipitated with glutathione-conjugated agarose beads and the presence of co-precipitated RBBP6-RING (the prey) was detected using a poly-clonal antibody raised against the RING finger of RBBP6. Our results show a clear interaction, which is significant when compared to background.

Attempts to repeat this assay the other way around—precipitating GST-RBBP6-RING and detecting with an antibody against MDM2-RING—failed because the anti-MDM2-RING antibody was found to have been raised against the N-terminus of MDM2 and therefore did not recognise the RING finger domain of MDM2. This will therefore need to be repeated. Future repeats will take advantage of HA-tagged forms of RBBP6-RING and MDM2-RING, which have become available in the laboratory, for clean detection of co-precipitated proteins using anti-HA antibodies.

Use of isolated MDM2-RING as prey has been found to be problematic due to the poor stability of the fragment. Repeats will therefore be done using GST-MDM2-RING; in that case RBBP6-RING will be used as bait instead of GST-RBBP6-RING, since GST is well known to form homo-dimers. That in turn will necessitate immunoprecipitation of the bait rather than GST pull down, using either an anti-RBBP6-RING antibody or an anti-HA antibody combined with the HA-tagged form of the bait. Detection of GST-MDM2-RING would be most easily carried out using an anti-GST antibody.

References

1. Aggarwal R, Zhang T, Small EJ, Armstrong AJ. 2014. Neuroendocrine prostate cancer: subtypes, biology, and clinical outcomes. Journal of the National Comprehensive Cancer Network. 12:719-26.

2. Amemiya Y, Azmi P, Seth A. 2008. Autoubiquitination of BCA2 RING E3 ligase regulates its own stability and affects cell migration. Mol Cancer Res. 6:1385-96.

3. Aravind L, Koonin EV. 2000. The U box is a modified RING finger - a common domain in ubiquitination. Current Biology. 10:132-134.

4. Ballinger CA, Connell P, Wu Y, Hu Z, Thompson LJ,.Yin L, Patterson C, 1999. Identification of CHIP, a novel tetratricopeptide repeat-containing protein that interacts with heat shock proteins and negatively regulates chaperone functions. Molecular and Cellular Biology. 19(6):4535–4545.

5. Barak Y, Juven T, Haffner R, Oren M. 1993. mdm2 expression is induced by wild type p53 activity. The EMBO Journal. 12:461 -468

6. Belzile JP, Richard J,Rougeau N, Xiao Y,Cohen EA. 2010. HIV-1 Vpr Induces the K48-Linked Polyubiquitination and Proteasomal Degradation of Target Cellular Proteins To Activate ATR and Promote G2 Arrest. Journal of virology. 84 (7):3320–3330

7. Brodsky JL, McCracken AA. 1999. ER protein quality control and proteasome-mediated protein degradation. Semin Cell Dev Biol. 10:507–513.

8. Brooks CL, Gu W. 2006. p53 ubiquitination: MDM2 and beyond. Mol Cell. 21:307–315.

9. Chandu D, Nandi D. 2002. From proteins to peptides to amino acids: comparative genomics of enzymes involved in downstream events during cytosolic protein degradation. Appl. Genom. Proteom. 4:235–252.

10. Chen J, Tang H, Wu Z, Zhou C, Jiang T, Xue Y, Huang G, Yan D, Peng Z. 2013. Overexpression of RBBP6, alone or combined with mutant TP53, is predictive of poor prognosis in colon cancer. PLoS One. 8:e66524.

11. Cheng Q, Cross B, Li B, Chen L, Li Z, Chen J. 2011. Regulation of MDM2 E3 Ligase Activity by Phosphorylation after DNA Damage. Molecular and Cellular Biology. 23:4951–4963.

12. Chibi M, Meyer M, Skepu A, Rees DJG, Moolman-Smook JC, Pugh DJR. 2008. RBBP6 Interact with Multifunction Protein YB-1 through its RING Finger Domain, leading to Uiquitination and Proteosomal Degradation of YB-1. Journal of Biological Chemistry. 384:908-916.

13. Colgan DF, Manley JL. 1997. Mechanism and regulation of mRNA polyadenylation. Genes Dev. 11:2755–2766.

14. Cyr DM, Höhfeld J, Patterson C. 2002 Protein quality control: U-box-containing E3 ubiquitin ligases join the fold. Trends in Biochemical Science. 27:368-75.

15. Davies KJ. 2001. Degradation of oxidized proteins by the 20S proteasome. Biochimie. 83: 301–310.

16. Deshaies RJ, Joazeiro CA. 2009. RING domain E3 ubiquitin ligases. Annu. Rev. Biophysic. Biomolecular Structure. 78:399-434.

17. Di Giammartino DC, Li W, Ogami K, Yashinskie JJ, Hoque M, Tian B, Manley JL. 2014. RBBP6 isoforms regulate the human polyadenylation machinery and modulate expression of mRNAs with AU-rich 39 UTRs. Genes and Development. 28:2248–2260.

18. Dhillon AS, Hagan S, Rath O, Kolch W. 2007. MAP kinase signalling pathways in cancer. Oncogene. 26: 3279–3290.

19. Dye BT, Schulman BA. 2007. Structural mechanisms underlying posttranslational modification by ubiquitin-like proteins. Annu. Rev. Biophysic. Biomolecular Structure. 36:131-150.

20. Everett RD, Boutell C, McNair C, Grant L, Orr A. 2010. Comparison of the biological and biochemical activities of several members of the alpha herpesvirus ICP0 family of proteins. Journal of Virology 84 (7):3476-3487.

21. Gao S, Scott RE. 2002. P2P-R Protein Overexpression Restricts Mitotic Progression at Prometaphase and Promotes Mitotic Apoptosis. Journal of cellular physiology. 193:199–207.

22. Gao S, Witte M, Scott R. 2002. P2P-R protein localizes to the nucleolus of the interphase cells and the periphery of the chromosomes in mitotic cells, which show maximum P2P-R immunoreactivity. Journal Cell Physiology 191:145-154.

23. Garcin D, Marq JB, Strahle L,le Mercier P,Kolakofsky D.2002. All four Sendai Virus C proteins bind Stat1, but only the larger forms also induce its mono-ubiquitination and degradation.Virology. 295:256-265

24. Gatza ML,Dayaram T,Marriott SJ. 2007. Ubiquitination of HTLV-I Tax in response to DNA damage regulates nuclear complex formation and nuclear export. Retrovirology. 4(95):1-12

25. GE Healthcare Life Sciences. Superdex High-performance columns [Internet][cited 29 October 2015]. Available from www.gelifesciences.co.jp/catalog/pdf/18116379.pdf

26. George A .1995. A new method for isolating genes involved in the processing and presenatation of antigens to cytotoxic T cells. D Phil Thesis. University of Oxford.

27. Goldberg AL. 2003. Protein degradation and protection against misfolded or damaged proteins. Nature. 426: 895–899.

28. Han YH, Moon HJ, You BR, Park WH. 2009. The effect of MG132, a proteasome inhibitor on HeLa cells in relation to cell growth, reactive oxygen species and GSH. Oncology reports. 22:215-221.

29. Harms KL, Chen X. 2006. The functional domains in p53 family proteins exhibit both common and distinct properties. Cell Death and Differentiation. 13: 890-897

30. Harris SL, Levine AJ. 2005. The p53 pathway: positive and negative feedback loops. Oncogene. 24:2899–2908.

31. Hashizume R, Fukuda M, Maeda I, Nishikawa H, Oyake D, Yabuki Y, Ogata H, Ohta T. 2001. The RING hetero-dimer BRCA1-BARD1 is a ubiquitin ligase inactivated by a breast cancer-derived mutation. J Biol Chem. 24:14537-14540.

32. Hicke L. 2001. Protein regulation by monoubiquitin. Nat. Rev. Mol. Cell. Biol. 2:95–201

33. Hoppe T. 2005. Multiubiquitylation by E4 enzymes: 'one size' doesn't fit all. Trends Biochem Sci. 30:183–187.

34. Hunziker A, Jensen MH, Krishna S. 2010. Stress-specific response of the p53-Mdm2 feedback loop. BMC Systems Biology. 4:94

35. Kappo MA, AB E, Hassem F, Atkinson RA, Faro A, Muleya V, Mulaudzi T, Poole JO, Mckenzie J, Chibi M., Moolman-Smook JC, Rees DJG, Pugh DJR. 2011. Solution Structure of the RING Finger-like domain of Retinoblastoma Binding Protein-6 (RBBP6) Suggest if Functions as a U-Box. Journal of Biological Chemistry, 287:7146-7158.

36. Kohno K, Izumi H, Uchiumi T, Ashizuka M, Kuwano M. 2003. The pleiotropicfunctions of the Y-box-binding protein, YB-1. BioEssays: Molecular, cellular and developmental biology. 25(7):691-8.

37. Kulathu Y, Komander D. 2012. A typical ubiquitylation – the unexplored world of polyubiquitin beyond Lys48 and Lys63 linkages. Nature Reviews Molecular Cell Biology. 13:508–523.

38. Laemmli UK .1970. Cleavage of structural proteins during the assembly of the head of bacteriophage T4. Nature. 227: 680-5.

39. Lauber J, Handrick R, Leptihn S, Dürre P, Gaisser S. 2015. Expression of the functional recombinant human glycosyltransferase GalNAcT2 in Escherichia coli. Microbial Cell Factories (2015) 14:3-15

40. LeBron C, Chen L, Gilkes DM, Chen J. 2006. Regulation of MDMX nuclear import and degradation by Chk2 and 14-3-3. EMBO J. 25: 1196-206.

41. Lee SD, Moore Cl. 2014. Efficient mRNA Polyadenylation Requires a Ubiquitin-Like Domain, a Zinc Knuckle, and a RING Finger Domain, All Contained in the Mpe1 Protein. Molecular and Cellular Biology. 34(21):3955–3967.

42. Levine AJ. 1997. p53, the cellular gatekeeper for growth and division. Cell. 88:323-31.

43. Li L, Deng B, Xing G, Teng Y, Tian C and Cheng X, Yin X, Yang J, Gao X, Zhu Y, Sun Q, Zhang L, Yang X, He F. 2007. PACT is a negative regulator of p53and essential for cell growth and embryonic development. Proceedings of the National Academy of Sciences. 104:7951-7956.

44. Li M, Brooks l, Wu-Baer F, Chen D, Baer R, Gu W. 2003. Mono- Versus Polyubiquitination: Differential Control of p53 Fate by Mdm2. Science. 302:1972-1975

45. Liew CW, Sun H, Hunter T, Day CL. 2010. RING domain dimerization is essential for RNF4 function. Biochemistry Journal. 431: 23–29

46. Linke K, Mace PD, Smith CA, Vaux DL, Silke J, Day CL. 2008. Structure of the MD2/MDMX RING domain hetero-dimer reveals dimerisation is required for their ubquitylation in trans. Cell Death and Differentiation. 15:814-848.

47. Love IM, Grossman RS. 2012. It Takes 15 to Tango: Making Sense of the Many Ubiquitin Ligases of p53. Genes and Cancer. 20(40):1-15.

48. Lowe SW, Sherr CJ. 2003. Tumor suppression by Ink4a-Arf: progress and puzzles. Current Opinion in Genetics and Development 13:77-83.

49. Lutz M, Wempe F, Bahr I, Zopf D, von Melchner H. 2006. Proteasomal degradation of the multifunctional regulator YB-1 is mediated by an F-Box protein induced during programmed cell death. FEBS letters. 580(16):3921-30.

50. Marianayagam NJ; Sunde M; Matthews JM. 2004. The power of two: Protein dimerisation in biology. TRENDS in Biochemical Sciences. 29(11)618-625

51. Messaoudi S, Peyrat JF, Brion JD, Alami M. 2008. Recent advances in Hsp90 inhibitors as antitumor agents. Anticancer Agents Med Chem. 8:761-82.

52. Metzger MB, Pruneda JN, Klevit RE, Weissman AM. 2014. RING-type E3 ligases: Master manipulators of E2 ubiquitin-conjugating enzymes and ubiquitination. Biochimica et Biophysica Acta. 1843: 47–60.

53. Meyer M, Morgenstern B. 2003. Characterization of gelatine and acid soluble collagen by size exclusion chromatography coupled with multi angle light scattering (SEC-MALS). Biomacromolecules. 4(6):1727-1732.

54. Miotto B, Chibi M, Xie P, Koundrioukoff S, Moolman-Smook H, Pugh D, Debatisse M, He F, Zhang L. 2014. The RBBP6/ZBTB38/MCM10 axis regulates DNA replication and common fragile site stability. Cell Reports 7:575–587.

55. Moela P, Choene MMS, Motadi LR. 2014. Silencing RBBP6 (Retinoblastoma Binding Protein 6) sensitises breast cancer cells MCF7 to staurosporine and camptothecin-induced cell death. Immunobiology. 219:593–601.

56. Morisaki T, Yashiro M, Kakehashi A, Inagaki A, Kinoshita H, Fukuoka T, Kasashima H, Masuda G, Sakurai K, Kubo N, Muguruma K, Ohira M,Wanibuchi H, Hirakawa K. 2014. Comparative proteomics analysis of gastric cancer stem cells. PLoS One. 9(11):e110736.

57. Nandi D, Tahiliani P, Kumar A, Chandu D. 2006. The ubiquitin-proteasome system. J. Biosci. 31:137-55.

58. Nathan JA, Kim HT, Ting L, Gygi SP, Goldberg AL. 2013. Why do cellular proteins linked to K63-polyubiquitin chains not associate with proteasomes? The EMBO Journal. 32: 552-565

59. Nikolay R, Wiederkehr T, Rist W, Kramer G, Mayer MP, Bukau B. 2004. Dimerization of the Human E3 Ligase CHIP via a Coiled-coil Domain Is Essential for Its Activity. Journal of Biological Chemistry. 279:2673-2678.

60. Okamoto K, Kashima K, Pereg Y, Ishida M, Yamazaki S, Nota A, Teunisse A, Migliorini D, Kitabayashi I, Marine JC, Prives C, Shiloh Y, Jochemsen AG, Taya Y. 2005. DNA damage-induced phosphorylation of MDMX at serine 367 activates p53 by targeting MDMX for MDM2-dependent degradation. Molecular Cell Biology. 25:9608-20.

61. Ogawa Y, Ono T, Wakata Y, Okawa K, Tagami H, Shibahara KI. 2005. Histone variant macroH2A1.2 is mono-ubiquitinated at its histone domain. Biochem Biophys Res Commun. 336(1):204-209.

62. Pickart CM, Cohen RE, 2004 Proteasomes and their kin: proteases in the machine age. Nat. Review Molecular Cell Biology. 5 177–187.

63. Pickart CM, Eddins MJ. 2004. Ubiquitin: structures, functions, mechanisms. Biochim. Biophys. Acta. 1695:55-72.

64. Pugh DJR, AB E., Faro A, Lutya PT, Hoffmann E, Rees DJG. 2006. DWNN, a novel ubiquitin-like domain, implicates RBBP6 in mRNA processing and ubiquitin-like pathways. BMC Structural Biology. 6:1.

65. Sakai Y, Saijo M, Coelho K, Kishino T, Niikawa N, Taya Y. 1995. cDNA Sequence and Chromosomal Localization of a Novel Human Protein, RBQ-1 (RBBP6), That Binds to the Retinoblastoma Gene product. Genomics. 30:98-101.

66. Semple CA, RIKEN GER Group, GSL Members. 2003. The comparative proteomics of ubiquitination in mouse. Genome Res. 13:1389–1394.

67. Shi Y, Di Giammartino DC, Taylor D, Sarkeshik A, Rice WJ, Yates JR 3rd, Frank J, Manley JL. 2009. Molecular architecture of the human pre-mRNA 3_-processing complex. Molecular Cell. 33:365–376

68. Shu KX, Li B, Wu LX. 2007. The p53 network: p53 and its downstream genes. Colloids Surf B Biointerfaces. 55(1):10-8.

69. Simons A, Melamed-Bessudo C, Wolkowicz R, Sperling J, Sperling R, Eisenbach L, Rotter V. 1997. PACT: cloning and characterization of cellular p53 binding protein that interacts with with RB. Oncogene. 14:145-155.

70. Singh CR, Asano K. 2007. Localization and characterization of protein-protein interaction sites. Methods Enzymol. 429:139–161.

71. Stommel JM, Wahl GM. 2004. Accelerated MDM2 auto-degradation induced by DNA-damage kinases is required for p53 activation. EMBO Journal. 23: 1547–1556.

72. Stone SL, Hauksdóttir H, Troy A, Herschleb J, Kraft E, Callis J. 2005. Functional Analysis of the RING-Type Ubiquitin Ligase Family of Arabidopsis. Plant Physiology. 137: 13–30.

73. Takaishi S, Okumura T, Wang TC. 2008. Gastric cancer stem cells. Journal of Clinical Oncology. 26:2876-2882.

74. Tanimura S, Ohtsuka S, Mitsui K, Shirouzu K, Yoshimura A, Ohtsubo M. 1999. MDM2 interacts with MDMX through their RING finger domains. FEBS Letter. 19:5-9.

75. Thrower JS, Hoffman L, Rechsteiner M, Pickart CM.2000. Recognition of the polyubiquitin proteolytic signal. The EMBO Journal. 19:94-102

76. Tollini LA, Zhang Y. 2012. p53 Regulation Goes Live—MDM2 and MDMX Co-Star: Lessons Learned from Mouse Modeling Genes and Cancer. 3:219–225.

77. Vo LT, Minet M, Schmitter JM, Lacroute F, and Wyers F. 2001. Mpe1, a zinc knuckle protein, is an essential component of yeast cleavage and polyadenylation factor required for the cleavage and polyadenylation of mRNA. Molecular Cell Biology. 21:8346–8356.

78. Vogelstein B, Lane D, Levine AJ. 2000. Surfing the p53 network. Nature. 408:307-10.

79. Wang X, Wang J. Jiang X. 2011. MDMX Protein is essential for MDM2 Protein-mediated p53 Polyubiquitination. The Journal of Biological chemistry. 286(27):23725-23734.

80. Weissman AM. 2001. Themes and variations on ubiquitylation. Nat Rev Mol Cell Biol. 2(3):169-78.

81. Wilkinson KD, Ventii KH, Friedrich KI, Mullay JE. 2005. The ubiquitin signal: assembly, recognition and termination. EMBO reports. 6:815–820.

82. Witte MM, Scott RE. 1997. The proliferation potential protein-related (P2P-R) gene with domains encoding heterogeneous nuclear ribonucleoprotein associated and RB1 binding shows repressed expression during terminal differentiation. Proceedings of the National Academy of Sciences of the United States. 94:1212-1217.

83. Woelk T, Sigismund S, Penengo L, Polo S. 2007. The ubiquitination code: a signalling problem. Cell Division. 2:1-12

84. Yamada K, Muramatsu M, Saito D, Sato-Oka M, Saito M, Moriyama T, Saitoh H. 2012. Characterization of the C-terminal diglycine motif of SUMO-1/3. Bioscience, Biotechnology, and Biochemistry. 76:1035-7.

85. Yin Q, Lamothe B, Darnay BG, Wu H. 2009. Structural basis for the lack of E2 interaction in the RING domain of TRAF2. Biochemistry. 48: 10558–10567

86. Yoshitake Y, Nakatsura T, Monji M, Senju S, Matsuyoshi H, Tsukamoto H, Hosaka S, Komori H, Fukuma D, Ikuta Y, Katagiri T, Furukawa Y, Ito H, Shinohara M, Nakamura Y, Nishimura Y. 2004. Proliferation Potential-Related Protein, an Ideal Esophageal Cancer Antigen for Immunotherapy, Identified Using Complementary DNA Microarray Analysis Clinical Cancer Research. 10:6437–6448.

87. Zhang L, Xu M, Scotti E , Chen Z, Tontonoz P. 2013. Both K63 and K48 ubiquitin linkages signal lysosomal degradation of the LDL receptor. Journal of Lipid Research. 54:1410-1420.

88. Zhao J, Hyman L, Moore C. 1999. Formation of mRNA 30 ends in eukaryotes: mechanism, regulation, and interrelationships with other steps in mRNA synthesis. Microbiol. Molecular Biology. Review. 63:405–445.

89. Zheng L, Lee WH. 2001.The retinoblastoma gene: a prototypic and multifunctional tumor suppressor. Experimental Cell Research. 264:2-18.

Appendix: Analysis of DNA sequencing of R3 mutants

```
cgcaccgccctgctggaatcggacgaacatacctgcccgacgtgtcaccaaaatgatgtt
 R  T  A  L  L  E  S  D  E  H  T  C  P  T  C  H  Q  N  D  V
agtccggacgcactgattgctaacaaatttctgcgccaggctgtcaataacttcaaaaac
 S  P  D  A  L  I  A  N  K  F  L  R  Q  A  V  N  N  F  K  N
gaaacgggctacacgaaacgtctgcgtaaacaa
 E  T  G  Y  T  K  R  L  R  K  Q
```

Translated DNA sequence indicating the three mutated residues: asparagine (N), lysine (K) and phenylalanine (F).

N312D

A

```
Query  1737   AAAGATATCATGACGGACGCAGTGGTTATTCCGTGCTGTGGTAATTCATATTGCGATGAA   1796
              ||||||||||||||||||||||||||||||||||||||||||||||||||||||||||||
Sbjct  284    AAAGATATCATGACGGACGCAGTGGTTATTCCGTGCTGTGGTAATTCATATTGCGATGAA   225

Query  1797   TGTATCCGCACCGCCCTGCTGGAATCGGACGAACATACCTGCCCGACGTGTCACCAAAAT   1856
              ||||||||||||||||||||||||||||||||||||||||||||||||||||||||||||
Sbjct  224    TGTATCCGCACCGCCCTGCTGGAATCGGACGAACATACCTGCCCGACGTGTCACCAAAAT   165

Query  1857   GATGTTAGTCCGGACGCACTGATTGCTAACAAATTTCTGCGCCAGGCTGTCAATAACTTC   1916
              ||||||||||||||||||||||||||||   ||||||||||||||||||||||||||||
Sbjct  164    GATGTTAGTCCGGACGCACTGATTGCTGACAAATTTCTGCGCCAGGCTGTCAATAACTTC   105

Query  1917   AAAAACGAAACGGGCTACACGAAACGTCTGCGTAAACAAcatcatcatcatcatcatTAA   1976
              ||||||||||||||||||||||||||||||||||||||||||||||||||||||||||||
Sbjct  104    AAAAACGAAACGGGCTACACGAAACGTCTGCGTAAACAACATCATCATCATCATCATTAA   45

Query  1977   TAACTCGAGCGGCCGCATCGTGACTGACTGACGATCTGCCTCGCG   2021
              ||||||||||||||||||||||||||||||||||||||||| |||||
Sbjct  44     TAACTCGAGCGGCCGCATCGTGACTGACTGACGATCTGC-TCGCG   1
```

B

(**A**) Query represents the expected sequence of the wild type and the subject (Sbjct) an experimental sequence read from the mutant construct. The mutated codon is shown in red. AAC in the wild type codes for asparagines (N) and GAC in the mutant for aspartic acid (D). (**B**) DNA sequencing traces were generated using SnapGene (GSL Biotech; available at snapgene.com): Sequencing was carried out from the 3'-end and hence the trace

corresponds to the reverse compliment of Sbjct- an arrow indicates the reverse codon of GAC.

<mark>K313E</mark>

A

```
Query  1747   TGACGGACGCAGTGGTTATTCCGTGCTGTGGTAATTCATATTGCGATGAATGTATCCGCA   1806
              ||||||||||||||||||||||||||||||||||||||||||||||||||||||||||||
Sbjct  280    TGACGGACGCAGTGGTTATTCCGTGCTGTGGTAATTCATATTGCGATGAATGTATCCGCA   221

Query  1807   CCGCCCTGCTGGAATCGGACGAACATACCTGCCCGACGTGTCACCAAAATGATGTTAGTC   1866
              ||||||||||||||||||||||||||||||||||||||||||||||||||||||||||||
Sbjct  220    CCGCCCTGCTGGAATCGGACGAACATACCTGCCCGACGTGTCACCAAAATGATGTTAGTC   161

Query  1867   CGGACGCACTGATTGCTAAC<mark>AAA</mark>TTTCTGCGCCAGGCTGTCAATAACTTCAAAAACGAAA   1926
              ||||||||||||||||||||   |||||||||||||||||||||||||||||||||||||
Sbjct  160    CGGACGCACTGATTGCTAAC<mark>GAA</mark>TTTCTGCGCCAGGCTGTCAATAACTTCAAAAACGAAA   101

Query  1927   CGGGCTACACGAAACGTCTGCGTAAACAAcatcatcatcatcatcatTAATAACTCGAGC   1986
              ||||||||||||||||||||||||||||||                  |||||||||||||
Sbjct  100    CGGGCTACACGAAACGTCTGCGTAAACAACATCATCATCATCATCATTAATAACTCGAGC   41

Query  1987   GGCCGCATCGTGACTGACTGACGATCTGCCTCGCG   2021
              |||||||||||||||||||||||||||||| |||||
Sbjct  40     GGCCGCATCGTGACTGACTGACGATCTGCTTCGCG   6
```

B
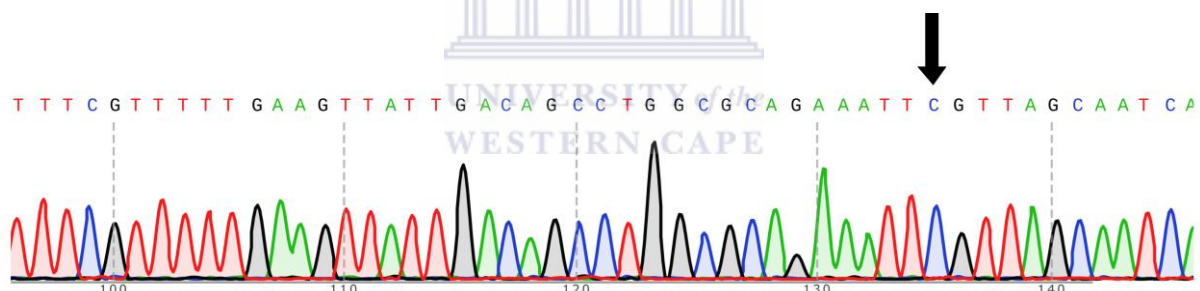
(**A**) Query represents the expected sequence of the wild type and the subject (Sbjct) an experimental sequence read from the mutant construct. The mutated codon is shown in red. AAA in the wild type codes for lysine (K) and GAA in the mutant for glutamic acid (E). (**B**) DNA sequencing traces were generated using SnapGene (GSL Biotech; available at snapgene.com): Sequencing was carried out from the 3'-end and hence the trace corresponds to the reverse compliment of Sbjct- an arrow indicates the reverse codon of GAA.

<mark>F314W</mark>

A

```
Query  1734   TGTAAAGATATCATGACGGACGCAGTGGTTATTCCGTGCTGTGGTAATTCATATTGCGAT   1793
              ||||||||||||||||||||||||||||||||||||||||||||||||||||||||||||
Sbjct  288    TGTAAAGATATCATGACGGACGCAGTGGTTATTCCGTGCTGTGGTAATTCATATTGCGAT   229

Query  1794   GAATGTATCCGCACCGCCCTGCTGGAATCGGACGAACATACCTGCCCGACGTGTCACCAA   1853
              ||||||||||||||||||||||||||||||||||||||||||||||||||||||||||||
```

```
Sbjct   228   GAATGTATCCGCACCGCCCTGCTGGAATCGGACGAACATACCTGCCCGACGTGTCACCAA   169

Query   1854  AATGATGTTAGTCCGGACGCACTGATTGCTAACAAATTTCTGCGCCAGGCTGTCAATAAC   1913
              ||||||||||||||||||||||||||||||||||||||| ||||||||||||||||||||
Sbjct   168   AATGATGTTAGTCCGGACGCACTGATTGCTAACAAATGGCTGCGCCAGGCTGTCAATAAC   109

Query   1914  TTCAAAAACGAAACGGGCTACACGAAACGTCTGCGTAAACAACATCATCATCATCATCAT   1973
              |||||||||||||||||||||||||||||||||||||||||||||||||||||||||||
Sbjct   108   TTCAAAAACGAAACGGGCTACACGAAACGTCTGCGTAAACAACATCATCATCATCATCAT   49

Query   1974  TAATAACTCGAGCGGCCGCATCGTGACTGACTGACGATCTGC   2015
              ||||||||||||||||||||||||||||||||||||||||||
Sbjct   48    TAATAACTCGAGCGGCCGCATCGTGACTGACTGACGATCTGC   7
```

B
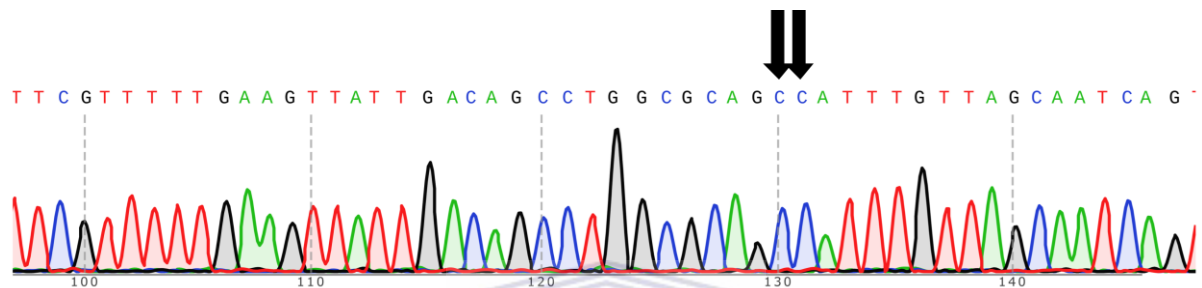
(**A**) Query represents the expected sequence of the wild type and the subject (Sbjct) an experimental sequence read from the mutant construct. The mutated codon is shown in red. TTT in the wild type codes for phenylalanine (F) and TGG in the mutant for tryptophan (W). (**B**) DNA sequencing traces were generated using SnapGene (GSL Biotech; available at snapgene.com): Sequencing was carried out from the 3'-end and hence the trace corresponds to the reverse compliment of Sbjct- an arrow indicates the reverse codon of TGG.